

23

New Energy Times Archive



Lawrence Livermore National Laboratory

September 14, 1989

Mr. John R. Huizenga
Co-Chairman of the Cold Fusion Panel
Energy Research Advisory Board
U.S. Department of Energy
1000 Independence Avenue, S. W.
Washington, D. C. 20585

Dear Mr. Huizenga:

We are pleased to send you our report "LLNL Research on Cold Fusion", covering the findings of numerous groups engaged in these activities over the last six months. Should you have further questions on this material please feel free to call.

Sincerely yours,

Keith I. Thomassen
Deputy Associate Director
for MFE Experiments

copy to: P. Coyle
C. Gatrousis
A. Glass
J. Holzrichter
B. Tarter

KIT/cl
kt993

LLNL Research on Cold Fusion

Scientific Editors: K.I. Thomassen and J.F. Holzrichter

Contributors: F.T. Aldridge, B. Balke, J. Bowers, D.B. Bullen,
M.D. Cable, M. Caffee, R. B. Campbell, C. Colmenares,
A. Connor, R.J. Contolini, L. Cox, A. Delucchi, J. Emig,
J.C. Farmer, O. Fackler, G.E. Gdowski, R.S. Glass,
W. G. Halsey, C.D. Henning, E.B. Hooper, B. Hudson,
M.Y. Ishikawa, S.M. Lane, E.R. Mapoles, R.D. McCright,
M. Mugge, R. Nagle, L.J. Perkins, M. Ruggieri, D.R. Slaughter,
C. Souers, K.I. Thomassen, R. Tsugawa, R.A. Van Konynenburg,
and R. M. White

September 14, 1989

Lawrence
Livermore
National
Laboratory

This is an informal report intended primarily for internal or limited external distribution. The opinions and conclusions stated are those of the author and may or may not be those of the Laboratory.

Work performed under the auspices of the U.S. Department of Energy by the Lawrence Livermore National Laboratory under Contract W-7405-Eng-48.

Contents

| | <i>Page No.</i> |
|--|-----------------|
| I. Overview..... | 2 |
| II. Summary..... | 3 |
| Appendix A: Electrolytic Cell Experiments..... | 8 |
| Appendix B: Electrolytic Cell and High-Pressure Gas Cell Experiments..... | 28 |
| Appendix C: Limits on Cold Fusion in Metal Hydride Systems under High Gas Pressure..... | 32 |
| Appendix D: Helium and Tritium Analyses..... | 40 |
| Appendix E: A Study of "Cold Fusion" in Deuterated Tritium Subjected to High Current Densities..... | 45 |
| Appendix F: Surface Analysis of Palladium Wire..... | 60 |

230 mA/cm² and showing similar null results. Analysis of the wire from the second experiment showed no helium buildup. In both cases, the thermometry "might" have missed seeing excess heat at the 10% level.

Another cell prepared similar to the cell described above was set up for sensitive neutron counting. The cell ran for 167 hours. It featured a proton recoil telescope detector that eliminated all background counts, and it used a very sensitive liquid scintillator (7% efficiency, absolutely calibrated, with neutron/gamma pulse-shape discrimination). These detectors set a limit of 0.2 neutrons/s from the 27-g Pd wire, which is half the level reported by S.E. Jones at Brigham Young University (BYU) with a 5-g sample and is a level inconsistent with electrolytic fusion power generation. Appendix A describes these results in more detail.

Other sets of experiments using electrolytic cells were run by a second independent group at LLNL, as described in Appendix B. This group's experiments were "category (b)" experiments, using our nomenclature, as were most of the other experiments described in this summary. They were designed to set a limit on fusion power production. The experiments tested for helium buildup in Pd and for neutrons. Null results were found by this group.

Collaboration with Texas A&M

We analyzed samples of Pd (see Appendix D) from a cell run at Texas A&M by S. Srinivasan. They reported 340-mW heat generation with their sensitive microcalorimeter with 300-mW heat input, indicating excess heat generation of 40 mW. However, it should be remembered that an additional power input of 150 mW was needed to separate the D₂O molecules. (The total electrical power input was 450 mW.) There was, however, no helium

generated in the Pd wire to the level of 3×10^5 atoms of ^3He and 5×10^8 atoms of ^4He in a sample of about 20 mg. The ^3He level is 10 orders of magnitude below the level associated with 40 mW of fusion power for 100 hours. An analysis of the electrolyte before and after the run showed no change in the tritium level in the original electrolyte. Surface analysis with Auger electron spectroscopy and secondary ion mass spectroscopy (SIMS) techniques revealed a substantial layer of material (Ca, C, Fe, O, Cl, Li, N, Cu, and traces of other elements) plated out on the Pd surfaces. These gave no clue as to possible excess heat-generating mechanisms; however, they indicate suspicious additional electrochemical mechanisms.

Neutron Burst Experiments

Experiments using pressurized deuterium cylinders loaded with Ti in various forms, similar to the Frascati experiments, were carried out by two groups at LLNL, as described in Appendices B and C. In a large number of runs at Livermore, during temperature cycles from 77 K to room temperature, no neutron output was observed. More recently, with overall detector efficiency improved to 15%, with higher-pressure operation up to 60 atm, and with a pair of coincidence detectors incorporating burst-mode triggering in the detection circuits, one LLNL group observed a few events that could be bursts of a few hundred neutrons. The time of the bursts does not correlate with the temperature of the cylinder, which is contrary to data from Los Alamos National Laboratory (LANL). To place some confidence in the results, multiple detectors and coincident signal detection is necessary. We find less than 100 neutrons per burst (if they are real) as a limit on this system. This is well below the Frascati level and also below the much lower rate reported by LANL. Spurious signals often appear on one detector but not

Appendix A

Electrolytic Cell Experiments

D.B. Bullen, M.D. Cable, J.C. Farmer, G.E. Gdowski,
R.S. Glass, W.G. Halsey, C.D. Henning, E.B. Hooper,
S.M. Lane, E.R. Mapoles, R.D. McCright, K.I. Thomassen,
and R.A. Van Konynenburg,

Appendix A

Electrolytic Cell Experiments

Introduction

This report describes the electrolytic cell experiments by a group from the Chemistry and Materials Science, Laser Fusion, and Magnetic Fusion programs. The first very quick experiments were attempts to replicate the Pons/Fleischmann results, using Pd wires or rods and simple neutron detection schemes. More sophisticated comparative experiments with light and heavy water, and with better neutron detection instruments, followed. Closed-system calorimetry was not attempted.

Preliminary Experiments

One of the first experiments used a Pyrex electrochemical cell with a Pd cathode and a Pt anode spaced apart laterally. The cathode was made by spot-welding a 1-mm-diameter Pd lead wire to a cylindrical Pd pellet, 1.27 cm in diameter by 1.27 cm long, of mass 19.23 g. The Pd pellet had been purchased from Specialty Metals and Alloys, Grove City, Ohio, in July 1978, but no record of chemical analysis was available. A pellet from the same lot was therefore analyzed using energy-dispersive x-ray analysis. Only Pd peaks were found. The anode was made of Pt wire 1 mm in diameter.

The electrolyte was made up by mixing 100 g of 99.5% pure D_2SO_4 (Sigma Chemical Co., Lot #61F-0465) with 97.75% pure D_2O . The total solution volume was 1000 ml $\pm 5\%$, making a 1-M concentration. The D_2O had an initial tritium activity of 12.4 $\mu Ci/ml$.

The cell was set up in the basement of Bldg. 381, where several neutron detectors were available for monitoring. Nitrogen gas was bubbled through the solution to remove the evolved deuterium-oxygen mixture produced by electrolysis. The cell was powered by a Sorenson 50 V dc-30 A current-controlled power supply. The cell was operated with about 11 A of current and about 8 V measured between the electrodes.

Two liquid scintillator neutron detectors (T2 and T3) as well as two BF₃ neutron survey meters (BF₃-1 and BF₃-2) were placed essentially in contact with the outer cell wall. A silver activation detector (Ag) was later added to the array of neutron detectors. The characteristics of these detectors are described in Table A-1, which gives the intrinsic detector efficiencies for 2.45-MeV D-D fusion neutrons, the estimated detector solid angles, and the background count rates.

This experiment was run for about 14 hours, until it was observed that the spot weld had broken between the Pd pellet and the Pd lead wire, apparently as a result of deuterium charging. During this time, the neutron count rates did not rise above background on any of the detectors.

The minimum detectable neutron production rate was estimated. Ordinarily a detectable signal can be defined as one that is at least three standard-deviations (3σ) above the average background rate, assuming Poisson counting statistics. Of course, the longer the integration time, the smaller the random fluctuations are relative to the average background rate. Table A-1 gives the 3σ threshold of detectability in terms of neutrons/s for integration times of 1 hour, 1 day, and 1 week. In an uncontrolled environment, as existed with this experiment, detector systems (especially those involving high-gain amplification stages) cannot be expected to have stable background rates to better than a few percent over significant counting

Table A-1. Characteristics of neutron detectors used in cold fusion experiments.

| Detector ID | Description | Intrinsic efficiency | Solid angle | Background rate (cpm) | Minimum detectable signal (neutrons/s) | | | |
|--------------------|--|----------------------|-------------|-----------------------|--|--------------------|---------------------|-----------|
| | | | | | 3 - σ (1-hr) | 3 - σ (1-d) | 3 - σ (1-wk) | 10% Bckgd |
| T2 | BC517 liquid scintillator 9954 Thorn PMT | 40% | 10% | 1300 | 6 | 1 | 0.4 | 54 |
| T3 | BC517 liquid scintillator 9902 Thorn PMT | 40% | 10% | 5400 | 12 | 2 | 1 | 225 |
| BF ₃ -1 | BF ₃ ionization chamber neutron survey meter | 0.1% | 17% | 0.8 | 34 | 7 | 3 | 8 |
| BF ₃ -2 | BF ₃ ionization chamber neutron survey meter | 0.1% | 17% | 1.6 | 48 | 10 | 4 | 16 |
| Ag | Ag activation detector | 0.15% | 25% | 30 | 92 | 19 | 7 | 130 |
| PRC | Proton recoil counter Si charged particle detector | 0.01% | 3% | 0.0001 | 22 | 4 | 2 | 0.06 |
| PSD | BC501 liquid scintillator 9954 Thorn PMT | 7% | 9% | 0.07 | 0.3 | 0.06 | 0.02 | 0.02 |
| BYU | BC505 liquid scintillator ⁶ Li glass scintillators | 2% | 50% | 0.06 | 0.2 | 0.03 | 0.01 | 0.01 |

times. This is due to unquantified effects of temperature, humidity, barometric pressure, cosmic-ray flux, etc. The last column in Table A-1 gives the signal level required to exceed the background rate by 10%, an arbitrary but reasonable upper limit for background drift. To be conservative, detectability thresholds should be taken as the larger of the two numbers, 3σ or 10% greater than background. For detectors having relatively high background rates (T2, T3, BF₃-1, BF₃-2, and Ag), thresholds are limited by the background stability, especially for long integration times. For detectors that have low background rates (PRC and PSD, mentioned below), it is the Poisson noise that sets the threshold. Consideration of background stability has often been ignored by other workers in quoting detection thresholds.

The next experiment again made use of a Pyrex cell with a Pd cathode and a Pt anode. However, in this cell the Pd cathode was a rod 1.27 cm in diameter and 20.3 cm long, extending out the top of the cell, and the anode was a coaxially mounted helical coil of Pt wire. The solution was again made up of 1 M D₂SO₄ in 97.75% D₂O, bubbled with N₂. The cell was powered by the same power supply as in the previous experiment, but with a total current of 29 A. This experiment was again monitored by several neutron detectors, including a scintillator, BF₃ Bonner spheres, and activation detectors. It was run for about 50 hours, and the electrolyte was replenished as needed.

During this weekend run, one of the BF₃ counters showed an increasing background rate (going from about 0.8 cpm to almost 3 cpm). It was confirmed that this was indeed a background effect rather than a real signal when it was found that the signal did not scale properly with detector-cell distance. In addition, the effect was demonstrated to be due to the detector's elevated temperature because of its close proximity to the cell's

electrical power supply. When an electric fan was used to cool the detector, the background rate returned to its original value.

No signal on any detector during this experimental run was observed to be above the limits of detectability as given in Table A-1. Thus an upper limit of about 50 neutrons/s (for 1-hour integration times) could be set.

The experiment was terminated when more detailed information about the Utah experiments became available. We learned that LiOD had been used as the electrolyte in those experiments rather than D_2SO_4 and that the charging time for a 1.27-cm-diameter electrode would be very long. We also realized that the large-diameter rod protruding out of the cell would constitute a rapid diffusion path for loss of deuterium. When the power was turned off, gas was evolved from the Pd cathode. This was collected and analyzed and was found to be composed primarily of D_2 , with a smaller amount of H_2 and some air. We observed that the Pd cathode had swelled noticeably over the fraction of its length that had been submerged and that it had acquired a copper color. The swelling was no doubt due to the formation of β palladium deuteride, which has a larger lattice parameter than Pd. We surmised that the copper color came from vapor-phase attack of the large copper crocodile clamp attached to the top of the Pd cathode rod, well above the electrochemical cell. We resolved to use smaller-diameter cathodes in future experiments and to protect connections from attack by vapors, using longer pigtails.

Matched-Cell Experiments

The primary objective of the matched-cell experiments was to determine whether or not measurable quantities of fusion products such as 3He , 4He , and 3T are generated under conditions purported to induce "cold

fusion." Two well-known D-D fusion reactions were initially proposed by Fleischmann and Pons to explain their results [M. Fleischmann, B.S. Pons, and M. Hawkins. *J. Electroanal. Chem.* **261**, 301–8 (1989)]. The first produces one 1.01-MeV triton and one 3.02-MeV proton, for a total energy yield of 4.03 MeV or 6.4×10^{-13} J:



The second reaction produces one 0.82-MeV ^3He nucleus and one 2.45-MeV neutron, for a total energy yield of 3.27 MeV or 5.2×10^{-13} J:



Fleischmann and Pons also initially reported the observation of 2.225-MeV gamma rays that they believed came from radiative capture of some of the neutrons produced in reaction (2) by hydrogen in the light-water bath surrounding their cold fusion electrochemical cell:



Later on, after problems were pointed out with their radiometric results, the Utah researchers postulated another reaction, involving the formation of ^4He and release of the fusion energy as heat, without nuclear radiation.

With all the above reactions, fusion products would be produced. At a current density of 0.5 A/cm^2 on the Pd cathode, Fleischmann and Pons claimed to have generated 10 W of excess power per cm^3 of Pd for a period of

120 hours (a total of about 4.3×10^6 J). If fusion were responsible for the release of this claimed excess energy, the concentrations of fusion products that would result would be in the range of 10^{17} to 10^{18} per cm^3 of Pd. These concentrations are many orders of magnitude above the detection limits of vacuum fusion-mass spectrometry. Therefore, use of this analytical technique on the Pd would be a sensitive test of the "cold fusion" hypothesis. Use of a matching light-water cell would provide a control experiment.

The second objective of the matched-cell experiments was to determine whether there is in fact a significant heat output from an electrolytic cell consisting of a Pd cathode, a Pt anode, and an electrolyte consisting of 0.1 M LiOD in D_2O . The most precise method would be closed-cell absolute calorimetry. However, this method requires specialized equipment and, in general, is very rigorous, expensive, and time-consuming. On the other hand, the large heat outputs claimed by Fleischmann and Pons should be readily observable by less sophisticated methods. We decided to perform a matched-cell differential thermometry experiment. The concept was to fabricate two cells, as nearly identical as reasonably practicable, except that one would use 0.1 M LiOD in D_2O , while the other would use 0.1 M LiOH in H_2O . They would be constructed with a geometry such that the Pd cathodes would have maximum mass with minimum thickness, and with a shape that would facilitate continuous monitoring of their temperatures. By using both heavy-water and light-water cells, we would be able to control for purely chemical effects and would thereby be able to separate them from nuclear fusion effects, should the latter occur, since the probability of fusion would be much greater for deuterium nuclei than for hydrogen nuclei at the same separation distance.

First Matched-Cell Experiment

Experimental Design. Pyrex electrolytic cells were used. The electrodes were coaxial. Each Pd cathode was fabricated from 1-mm-diameter wire, wound in the shape of a helix, with one end extended in a pigtail for electrical connection. The two cathodes were made from the same original wire, which was made by swaging and drawing a Pd pellet from the same lot as the one used in the first and second preliminary experiments. The wire was cut into two pieces, nominally 60.9 cm long, with masses 5.86 ± 0.003 g and 5.89 ± 0.003 g. The submerged portion of each cathode consisted of 35.5 cm of wire, wound in a helix around a 0.48-cm-o.d. closed-end glass tube, forming 19 turns. The surface area of the submerged portion was 11.2 cm^2 , its volume was 0.279 cm^3 , and its mass was 3.36 g.

The electrolyte for the light-water cell was prepared by dissolving 2.395 g of LiOH in 1.00 liter of deionized H_2O , to make a 0.1-M solution. The heavy-water cell electrolyte was prepared by dissolving 0.748 g of LiD in 840 ml of D_2O , again making a 0.1 M solution. The heavy water was 97.75 at.% D vs D + H, as before. The LiOH was reagent grade, and the LiD was obtained from the Laser Program.

Each anode was made of Pt foil with an active area of about 100 cm^2 wrapped concentrically with the Pd cathode into a slotted cylinder about 2 cm in diameter.

A metal-sheathed Type K thermocouple was inserted into the closed-end glass tube inside each Pd helical cathode for temperature monitoring. A solid-state cold-junction compensator and linearizer was attached to each thermocouple, and the output was fed to a dual-input strip chart. Cell voltages were monitored using a second dual-input strip chart.

A BF₃ Bonner sphere-type neutron survey meter was placed about 1 m from the cells, only for hazard monitoring. Counts were accumulated on a scaler.

Identical current-controlled (galvanostatic) power supplies were used to power the two cells.

The thermocouples were calibrated using ice water and boiling water, and were accurate to within 0.1°C.

The diffusion time required to bring the D concentration to steady state for 1-mm wire samples was estimated from the equation $r^2 = Dt$, where r is the radius ($= 0.05$ cm) and D is the diffusion coefficient (5×10^{-7} cm²/s). The result was 1.4 hours. We resolved to charge the samples for times long compared to this to be sure that steady state had been achieved for the overpotential used.

We also performed a calculation to determine whether the total production of D by electrolysis during this time, using the current densities of Fleischmann and Pons, would be sufficient to equal the number of Pd atoms in the sample, and would thus be sufficient to provide 1-to-1 stoichiometry, should this be permitted thermodynamically. For a 1-mm-diameter Pd wire, with a current density of 90 mA/cm², sufficient D production would occur in 0.84 hours to produce 1-to-1 stoichiometry, assuming no D was lost to D₂ evolution. We resolved to operate at current densities of at least this value for times long compared to 0.84 hours, to account for D₂ evolution.

Procedure. The cells were first allowed to reach steady conditions at zero input current. Then the current through both cells was slowly raised to 1.00 A, held constant for 98 hours, then raised to 3.00 A for 21 hours, then to 5.00 A for 27 hours and finally turned off after a total of 146 hours. These currents corresponded to current densities of 0, 90, 270, and 450 mA/cm². The

electrolytes were replenished with H_2O and D_2O as needed. After the current was turned off, the Pd wires were removed from the cells in order to take samples from the bottom of each for surface analysis and for ^3He and ^4He analysis by vacuum fusion-mass spectrometry. After removal from the cells, the Pd wires were first rinsed with deionized water, then the samples were clipped off and placed in plastic bags, and the wires were placed on laboratory tissue to dry. After a short time (about one or two minutes), both wires heated to incandescence and burned the tissues on which they were resting. The samples that had been placed in plastic bags melted holes in the bags. After a few minutes, the wires and samples had cooled back to room temperature.

Results. The results of the first matched-cell experiment are shown in Table A-2 and Figure A-1. Note that there was no significant change in temperature of either cell once steady-state operation had been achieved at each current, except when the electrolyte was replenished. The neutron count rate also remained constant (Fig. A-2). The results of ^3He and ^4He analysis (by Rockwell) are shown in Table A-3. As can be seen, no ^4He was observed in either sample to within the uncertainty of the analysis. The detection limits were between 10^8 and 10^9 atoms of ^3He and ^4He per sample, corresponding to between 10^{10} and 10^{11} atoms per gram. A very small amount of ^3He was observed in the sample from the D_2O cell. The surface analysis (Appendix F) showed a variety of elements.

Discussion. It is clear that there is no evidence of nuclear fusion in this experiment. The small amount of ^3He observed in the Pd from the D_2O cell can be accounted for by charging of the Pd with the tritium initially present in the D_2O , followed by its radioactive decay to form ^3He . The observed heating

Table A-2. Matched-cell experiments.

| Run | Date | Time | Current (A) | | Voltage (V) | | Temp. (°C) | | Power (W) | |
|----------------------|------|-------|------------------|------------------|-------------------|-------------------|------------------|------------------|------------------|------------------|
| | | | H ₂ O | H ₂ O | D ₂ O | H ₂ O | D ₂ O | H ₂ O | D ₂ O | H ₂ O |
| #1 | 4-6 | 21:30 | 0 | 0 | 0 | 0 | 22 | 22 | 0 | 0 |
| (No water bath) | 4-7 | 17:00 | 0.9 | 0.9 | 4.7 | 4.1 | 32 | 35 | 4.2 | 3.7 |
| | 4-9 | 7:09 | 0.9 | 0.9 | 4.50 | 3.95 | 30 | 33 | 4.1 | 3.6 |
| | 4-11 | 16:09 | 3.0 | 3.0 | 5.35 | 4.75 | 54 | 58 | 16.1 | 14.3 |
| | 4-12 | 22:13 | 5.0 | 5.0 | ~5.4 ^a | ~4.0 ^a | 76 | 74 | ~27 ^a | ~20 ^a |
| #3 (No water bath) | 4-24 | 21:25 | 1.8 | 2.0 | 6.0 | 5.5 | 42 | 38 | 10.8 | 11.0 |
| #3 (Water bath used) | 4-25 | 10:20 | 2.0 | 2.0 | 5.7 | 5.6 | 32 | 26 | 11.4 | 11.2 |
| | 4-25 | 16:40 | 4.0 | 4.0 | 7.3 | 7.3 | 36 | 38.5 | 29.2 | 29.2 |
| | 5-8 | 8:03 | 4.0 | 4.0 | 6.6 | 6.8 | 35 | 36.5 | 26.4 | 27.2 |

^aVoltage trace lost; estimated from hand plot.Table A-3. Results of helium analysis of palladium by vacuum fusion-mass spectrometry from first matched-cell experiment.^a

| Cell | Sample no. | Sample mass (mg) ^b | Date of analysis | Measured helium (10 ⁹ atoms) | |
|------------------|------------|-------------------------------|------------------|---|-----------------------|
| | | | | ³ He (1 σ) | ⁴ He (1 σ) |
| H ₂ O | A | 16.97 | 4/18/89 | <0.1 (0.2) | <0.1 (0.3) |
| | B | 16.10 | 4/19/89 | <0.1 (0.2) | <0.1 (0.3) |
| D ₂ O | A | 14.93 | 4/19/89 | 0.7 (0.2) | 0.3 (0.3) |
| | B | 17.81 | 4/20/89 | 0.6 (0.2) | <0.1 (0.3) |

^aAnalysis performed by Brian Oliver, Rocketdyne Division, Rockwell Corp.^bMass uncertainty is ±0.01 mg.

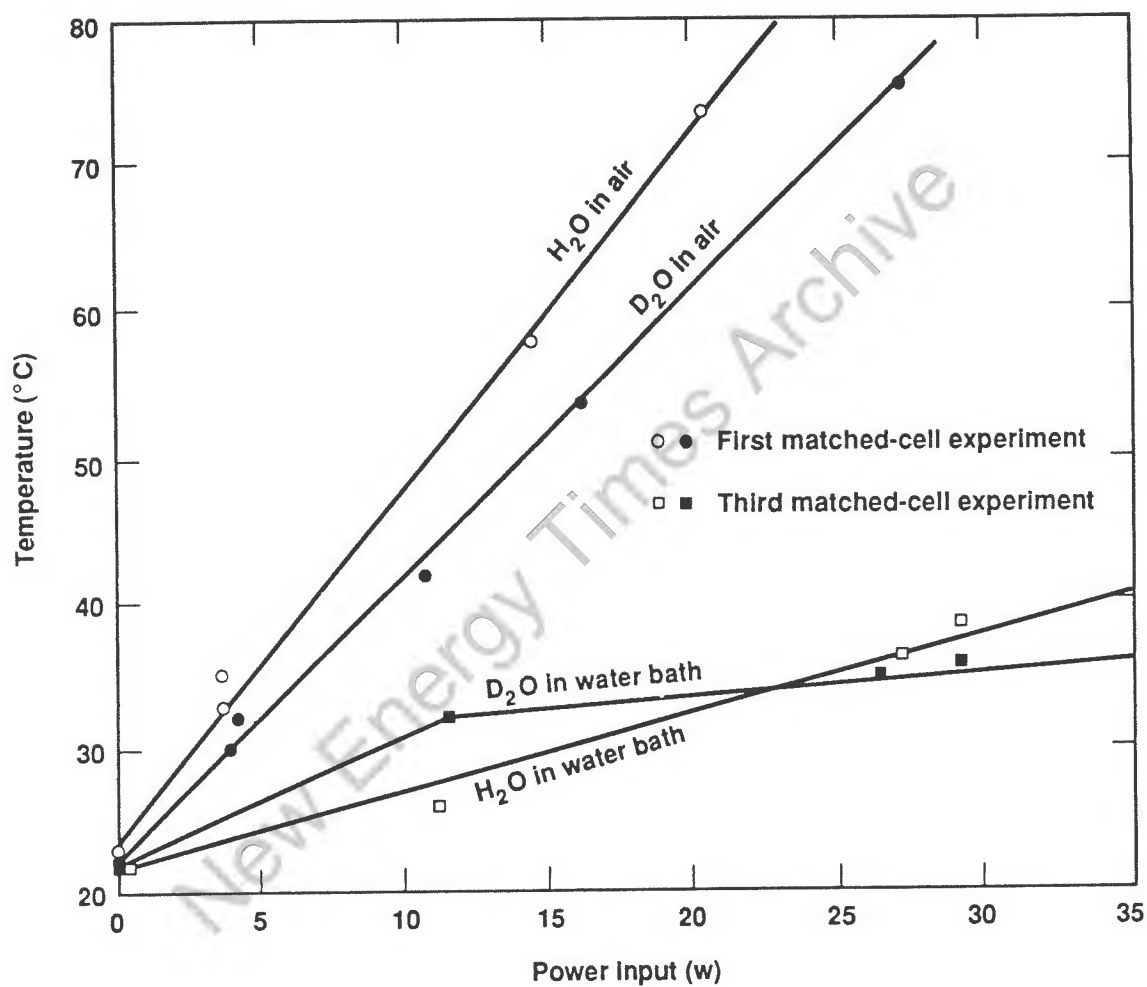


Figure A-1. Temperature vs total input power for matched-cell experiments.

Neutron Detector Data (1 meter)

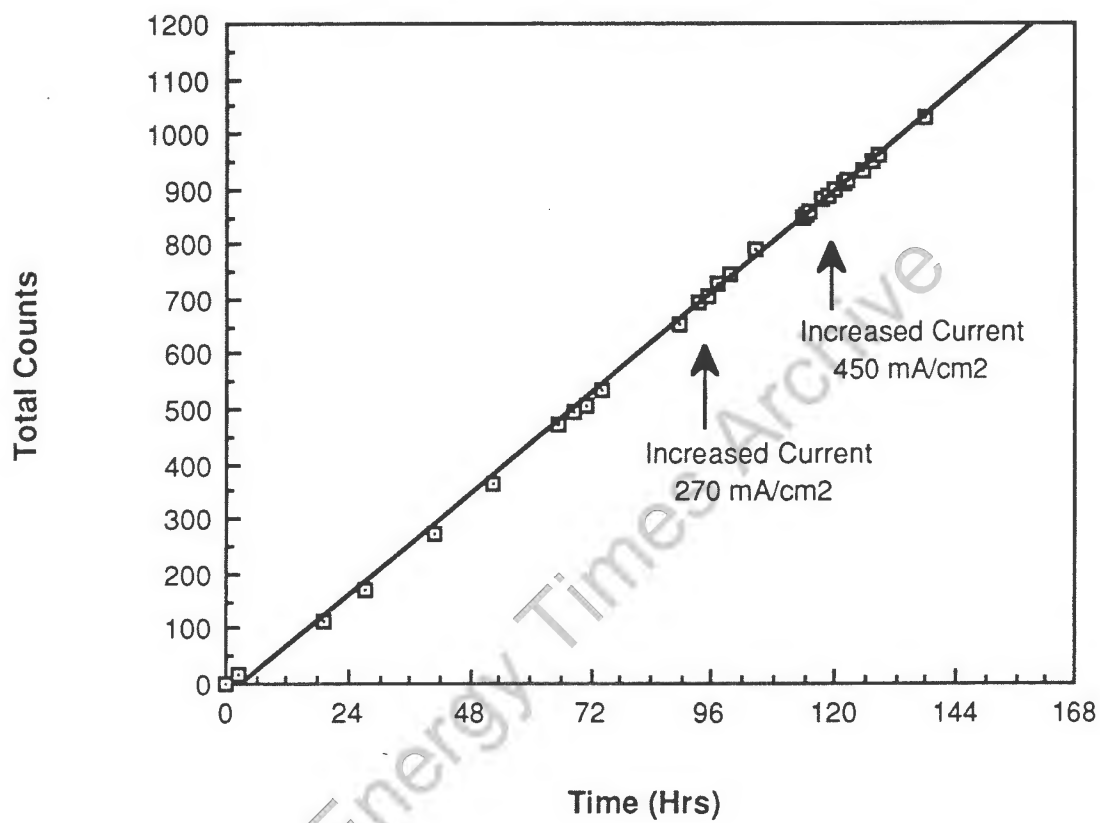


Figure A-2. Neutron-counting data from first matched-cell experiment.

to incandescence after removal from the cells can be explained as follows: When the electrochemical overpotential was removed, excess deuterium began to evolve from the Pd wires. Upon arrival at the surface of the Pd, it was catalytically oxidized to D_2O with oxygen from the air. This produced heat, which raised the temperature of the wire, raising the diffusion coefficient and lowering the solubility of D in Pd. Evolution of D thus increased, and an avalanche process occurred, heating the wire to red heat. When the D was exhausted, the wire cooled down.

The comparative absolute values of temperature in the two cells depend on their exact geometry and on the differences in thermal conductivity of the two solutions, so that undue significance should not be attached to them. The important observation is that no significant changes were observed once steady state had been achieved at each current.

Second Matched-Cell Experiment

Purpose. In view of the heating of the Pd wires after removal from the cells in the first matched-cell experiment, we decided to perform an experiment to determine whether a significant heat release could be observed in a cell by raising the cathode out of the electrolyte slightly after charging with H or D.

Experimental Design. The same configuration was used as in the first matched-cell experiment. The same Pd wires were used, less the amount removed for helium and surface analysis.

Procedure. The Pd cathodes were charged in both cells by passing a current of 3 A through the cells for 22 hours. Then the current was backed off to 1.5 A, the temperatures were allowed to stabilize, and the thermocouples were raised to the tops of the helical coils of the Pd cathodes. The top-most

coil windings were then raised above the electrolyte, and the temperatures were monitored.

Results. The temperatures dropped initially, and then rose back to ambient cell temperature. No significant positive temperature excursion was observed.

Discussion. In this configuration, the overall thermal conductance from the exposed portions of the Pd coils apparently remained sufficiently high that thermal runaway was prevented. This is perhaps not too surprising, since the coils were made of a pure metal and were relatively short in length, and the bottom ends were submerged in aqueous solutions.

Third Matched-Cell Experiment

Purpose. As the earlier matched-cell experiments were under way, information received from other researchers suggested that two of the conditions in our experiments might be precluding the achievement of nuclear fusion. The first was the possibility that the Pd cathodes contained sufficient initial concentrations of H and other impurities that the concentration of D was limited to values too low for significant fusion to occur. The second was that the heavy water we used was not sufficiently isotopically pure, so that the ingress of H into the Pd during the experiments prevented achievement of sufficiently high D concentration.

Information from Paul Coronado of our laboratory indicated that to do a thorough purging of H from the Pd, we would have to perform vacuum bake-out in a quartz tube furnace at 600°C for several hours, then drop to 300°C, bleed in D₂ gas to a pressure of 100 torr, pump it back out, and repeat the D₂ flushing process until the residual gas analysis showed only deuterium. After this, the Pd would have to be kept in inert atmosphere.

This would necessitate performing the electrochemical experiments in a flowing-argon glove box. Since this would require resources beyond those available within the scope of our ad hoc project, and since there was no indication that the Utah researchers had taken such precautions, we decided to simply perform a vacuum bake-out of some new Pd wires and keep them in an argon atmosphere until they were inserted into the cells.

We obtained a new supply of heavy water of higher isotopic purity.

Experimental Design. The design of the third matched-cell experiment was similar to that of the first two. The Pd cathodes were fabricated from another pellet, using the same starting material as before. The pellet was swaged and drawn to 1-mm-diameter wire. Two samples were cut from this wire, each 79.4 cm long. The masses were 8.065 ± 0.001 g and 8.032 ± 0.001 g, respectively. Helical coils of 28 turns, using 54.0 cm of length, were fabricated from one end of each wire, leaving a pigtail for electrical connection. The total submerged length was 55 cm, the total submerged surface area was 17.3 cm², and the total submerged volume was 0.432 cm³.

The electrolytes were prepared by adding LiD to D₂O and LiOH to deionized H₂O. Solutions of 0.1-M concentration LiOD in D₂O and LiOH in H₂O were made. The isotopic purity of the D₂O was 99.5% (Aldrich).

The Pd cathodes were baked out in vacuum for 3 hours at 600°C and were stored in argon gas until insertion into the cells. The Pt anodes were the same as before.

Matched current-controlled power supplies were again used, and neutrons were again monitored for safety purposes using a BF₃ Bonner sphere survey instrument.

The two cells were placed in a water bath, the temperature of which was not controlled but was monitored occasionally with a thermometer.

Procedure. After steady temperatures were achieved at zero current, the cell currents were raised to 2 A, equivalent to 116 mA/cm². After about 18 hours, the currents were increased to 4 A, equivalent to 232 mA/cm². The positions of the Pd cathodes were adjusted slightly relative to the anodes so that nearly the same total power input was used in both cells. The cells were operated for a total time of 414 hours. The electrolytes were replenished with H₂O and D₂O, respectively, as needed. Upon termination of the experiment, one of the Pd cathodes was quickly removed from its cell, dried, and inserted into an argon atmosphere while monitoring the temperature with the thermocouple. The thermocouple reading rapidly dropped from 24°C to 12°C, and the wire was subsequently found to be cold to the touch.

Results. Table A-2 and Figure A-1 show the results of the experiment. As in the first matched-cell experiment, no significant temperature differences were observed between the cells, and no significant temperature rises occurred, with the exception of one that was traced to a dead battery in the cold junction compensator. A rise in apparent neutron-counting rate was coincident with a significant rise in room temperature, resulting from failure of the building air conditioning, and was thus attributed to temperature rise of the survey meter.

Discussion. Again, no evidence for nuclear fusion was obtained. The drop in temperature upon removal of the Pd from the cell and insertion into an argon atmosphere can be attributed to the endothermic release of excess hydrogen from solution in the Pd. Without O₂ present, there is no overwhelming production of heat due to oxidation.

Experiment with Improved Neutron Counting

A final attempt was made to observe neutrons, this time from a newly designed cell. This cell consisted of a string of seven 0.5-in-dia. by 2-mm-thick Pd disks, separated by 2 mm and laser-welded onto a 1-mm Pd wire. The point of this design was to maximize the Pd mass in a small region to improve the counting geometry and at the same time to minimize the distances that deuterium needed to diffuse in order to reach saturation. The Pd disks were annealed for 3 hours at 600°C to reduce impurities and defects.

Two new neutron detectors were designed and built for this experiment by M. Cable, M. Nelson, G. Mant, and C. Bennett of the Laser Program. Both detectors had improved efficiency and lower background. One detector (PSD) was a liquid scintillator cell optimized for pulse-shape discrimination; that is, because neutrons produce pulses with slightly longer tails than gamma-rays, the substantial gamma-ray background can be identified and discarded. Gamma-rejection was of the order of 10^{-4} . This detector had a comparable detection threshold compared to the BYU detector (see the last row of Table A-1) using a source strength equivalent to that claimed by BYU. (Our electrolytic cell, however, contained several times the mass of the BYU cell and therefore should have produced a much larger signal.) The other detector (PRC) was a proton-recoil telescope consisting of an evacuated chamber in which a 1-mm-thick polyethylene radiator was positioned in front of a 20-mm-thick, 100 mm² silicon charged-particle detector, followed by another silicon charged-particle detector 400 mm thick and having an area of 450 mm². Neutrons entering the front of this detector can undergo an elastic scattering event with a proton in the polyethylene. The recoil proton can then pass through the first detector, losing a portion of its energy, and deposit its remaining energy in the second silicon detector. A

very low background can result by requiring a coincidence between the two detectors where the amount of energy deposited in each is consistent with a 2.45-MeV neutron interaction.

These detectors ran for 167 hours. The PRC registered only one count in this period. Again, no neutron signal from the electrolytic cell was observed to be above the detectable limits for these detectors as given in Table A-1.

New Energy Times Archive

Appendix B

Electrolytic Cell and High-Pressure Gas Cell Experiments

F.T. Aldridge, R.J. Contolini, M.Y. Ishikawa,
and D.R. Slaughter

Appendix B

Electrolytic Cell and High-Pressure Gas Cell Experiments

To date, eight cold fusion (CF) experiments have been done, half of which were heavy-water electrolysis experiments; the other half examined high-pressure metal-gas reaction phenomena. The experiments involving an electrolysis set-up base were variants on the Fleischmann-Pons and Jones et al. electrolysis cold fusion experiments, while the high-pressure cell work was related to that done at Frascati and at Los Alamos. Electrolysis experiments carried out between March and the end of May 1989 used palladium rods and palladium sheet of various total volumes ($\leq 15 \text{ cm}^3$) in a 0.1-M LiOD/D₂O electrolyte solution; the high-pressure cell experiments used both titanium filings and fine titanium mesh powder. Neutron diagnostics for both CF approaches included detailed neutron spectroscopy and neutron counting from three different detector systems (NaI, NE213, Stilbene). Data were collected on a specially modified Nuclear Chemistry-built data collection system—such as is used for long-time (month-scale) counting (of environmental samples, among others). Nuclear Chemistry also provided detailed mass spectroscopy and ion beam probe work of liquid and metal samples from our electrolysis experiments. Internal temperature and pressure readings were monitored on the Frascati-type experiments.

Results. Measurement of the helium isotope concentrations in the cathodes of our first and third electrolytic experiments, relative to "blank" material removed from these cathodes prior to use, indicated that no nuclear

reactions occurred in these materials, at levels 10^{10} times lower than those which should be present in the cathodes reported to have produced 4 MJ/cm^3 excess heat due to deuteron fusion, if the fusion reactions produced ^3He or ^4He . The electrolyte itself showed a 13% enrichment in tritium, but this was what would be expected from the electrolysis of the D_2O , using literature values for enrichment factors, so that no enrichment due to cold fusion was seen. Results of the ion beam-mass spectrometric probing of the surfaces of the Pd cathodes provide a key to understanding at least the reported electrolysis "cold fusion" excess heat phenomenon. We have seen no reproducible neutron generation which could be statistically attributed at high confidence to "cold fusion," either electrolytic or metal-gas.

A major setback to verifying the seemingly successful results obtained on CF at Los Alamos is the local lack of the four high-efficiency (34%), cavity-type detectors (each containing 18 ^3He tubes) with time resolutions of $\leq 200 \text{ ns}$. A special closed-system calorimeter needs to be designed for heavy-water electrolysis experiments. Closed-system calorimetry is necessary for proof or disproof of "excess heat," the second and more astonishing feature of the "cold fusion" phenomenon. (The Fleischmann-Pons type of experiments, which are not closed in this sense, have been widely criticized for their "open" feature.) Closed-system calorimetry is necessary to avoid large errors which can be introduced by the flow of electrolytically produced deuterium and oxygen out of the calorimeter cell. Although the volume of escaping gas can be measured, there are still errors introduced due to water vapor or liquid droplets entrained in the gas, lack of knowledge of the exact temperature of the gas, and the possibility that some of the hydrogen and oxygen could recombine within the cell. These errors are probably responsible for the wide range of values being published for excess energy in cold fusion experiments.

In a closed cell, a catalyst is used to recombine the hydrogen and oxygen, and the cell is completely sealed. Such a cell is being designed now, based partly on the cell developed by M. E. Hayden of the University of British Columbia. In this cell, an electrically heated palladium wire in the gas space above the heavy water is used as the catalyst. Once hydrogen and oxygen are being produced within the cell, the heat of recombination keeps the wire hot, and electrical heating is no longer needed. Since the net chemical reaction inside the cell is zero, the heat output of the cell should be the same as the electrical energy input for electrolysis if no cold fusion is occurring and if other reactions, such as lithium alloying with the electrodes, are negligible.

Appendix C

Limits on Cold Fusion in Metal Hydride Systems under High Gas Pressure

B. Balke, L. Cox, O. Fackler, M. Mugge, and R.M. White

Physics Department

J. Bowers, J. Emig, C. Souers, and R. Tsugawa

Chemistry and Material Sciences

Appendix C

Limits on Cold Fusion in Metal Hydride Systems Under High Gas Pressure

After the initial reports from Utah of fusion catalysis in electrolysis cells, i.e., "cold fusion," an independent line of investigation was initiated by a group of Italian cryochemists led by Scaramuzzi at the Frascati Institute. Assuming that the importance of electrolysis in the catalysis might simply be to drive the Pd-D system away from equilibrium, these researchers reasoned that fusion might also be enhanced if metal hydrides were subjected to high pressures and low temperatures. Indeed, their detectors recorded an apparent increase in neutron flux as titanium, under exposure to 50 atm D₂, was temperature-cycled between -197° and 0°C. Our efforts have been to check these results, as well as similar reports from other Italian laboratories and, more recently, from Menlove and coworkers at LANL.

The bulk of this report covers our attempts to reproduce the Frascati experiments and similar measurements done under 10 atm pressure at Genoa. The researchers at Frascati reported bursts of nearly 2×10^5 neutrons. Later, when the sample was evacuated and allowed to warm to room temperature, they saw a smooth rise in the count rate in their detector. The rate peaked after 10 hours at a level corresponding to the emission of nearly 5000 neutrons/s from their sample. We have seen neither of these effects. Our data allow us to set neutron production limits which are typically less than 1% of those reported at Frascati. The reports from LANL indicate extremely short bursts of 100 or so neutrons, and steady-state production rates

of a few per minute. Our attempts to verify these results are as yet inconclusive, but a limited program of improvements will enable us to make sensitivity at these levels.

Description of the Experiment

Our experiment consists of a high-pressure gas system feeding a cell which contains a metallic getter of hydrogen. The cell was placed in a dewar and automatically cycled between liquid nitrogen and room temperatures. Gas pressure and internal and external temperature readings were made every 30 seconds. Photomultiplier tubes coupled to 5-cm-thick \times 12.5-cm-diameter cylinders of fast plastic scintillator were used to monitor the radiation flux from the gas cell. Two independent detectors were in operation at all times. Our detectors produced short pulses (approximately 10 ns) which did not permit rejection of gamma radiation backgrounds using the standard pulse-shape discrimination technique. To reduce this background, we surrounded the gas cell and detectors with 4 inches of lead shielding. We also calibrated our detectors to allow selection of the energy range most sensitive to 2.5-MeV D-D fusion neutrons. This decreased the neutron detection efficiency by 40% but reduced our backgrounds by a factor of seven. In the final configuration, the background count rate was typically 1.3/s in either tube. This high background rate was offset by a high neutron detection efficiency (4%) as compared to the Frascati apparatus (0.01%).

The detectors were calibrated using a ^{22}Na gamma source. Conversion between the gamma and neutron energy scales was accomplished using published measurements of the light output of plastic scintillator. A ^{252}Cf source was used to verify that the detectors responded to neutrons. The detector efficiency was calculated by Monte Carlo computer simulation using

the known neutron-proton cross section at 2.5 MeV and the hydrogen density in plastic. A correction factor of 0.6 was included in the efficiency calculation to account for cuts on the proton recoil energy (described below).

The signals generated by the phototubes were analyzed in two ways. First, all pulses corresponding to proton recoil energies above 300 keV were analyzed by a charge-integrating ADC and histogrammed in 8-s intervals. Since the ADC conversion time was typically 120 μ s, this data was not sensitive to short bursts of neutrons. With a second trigger, the number of events with energy greater than 1 MeV was accumulated in 1-s steps. This energy cut eliminated the bulk of the background from natural radioactivity. A typical run commenced with 30–60 minutes of background data, followed by introduction of D₂ gas and 10–90 hours of signal data. After the run was over, the energy histograms were integrated over the range from 1.0 to 3.5 MeV, and the resulting rates were examined for evidence of steady-state fusion, i.e., any significant increase in the rate over background. This count rate was also histogrammed vs cell temperature. If a fluctuation in the rate was seen, the energy spectrum in that interval was examined for an excess of events with energies between 1.0 and 2.5 MeV. The second trigger sample was simply searched for large bursts. No rate increases were observed which could not be correlated with external sources, i.e., radioactive sources or natural radioactivity when the lead shielding was partially dismantled. We therefore obtain fusion limits from each run. The results of our preliminary analysis, as given in Table C-1, are quite conservative. Fusion occurring at these levels would have increased the count rate by five standard deviations.

Procedure and Results

A summary of the experiment is presented in Table C-1. For safety reasons, the gas pressure was limited to 10 atm D_2 prior to construction of a high-pressure cell. The shakedown run, using vanadium powder, was executed before lead shielding had been installed and suffered from backgrounds nearly 30 times higher than in later runs. After adding lead shielding and changing our detector configuration, we began an extended cycle of runs using titanium as the host material. The Frascati results stimulated many questions. Is the observed result a surface or bulk effect? Is the rate of deuterium permeation a critical parameter? During these runs we varied the sample preparation and controlled the exposure to deuterium in an attempt to explore these possibilities. Temperature-cycling of the cell was begun with the second of our titanium samples. The third sample was pressurized to 50 atm, as in the Frascati procedure. In all cases, after one to three days under pressure, the cell was cooled, the deuterium was removed, and data-taking was continued for 5–30 hours without any further cooling. We also conducted runs using unannealed and annealed palladium as the host. In this case, we followed the procedure outlined by Ricci and coworkers at the May 1989 fusion workshop in Varenna, Italy. No cooling was performed, but the cell was evacuated and heat after a half-day exposure to D_2 . Based on the presentations made at the Varenna meeting, neutron yields should have been similar to those obtained with titanium as the host material. Again, we saw no evidence for neutron production above background levels.

Although indicating that the original cold fusion yields were unlikely to be upheld, presentations at the May conference in Santa Fe still held out tantalizing promise that cold fusion might be taking place at much lower

levels. Although our detectors are not sensitive to the extremely low steady-state production levels quoted by Jones and others, we recognized that we could potentially detect short bursts of 100–300 neutrons as observed by Menlove and coworkers at LANL. Increasing the thickness of our scintillator three-fold (to 6 inches), we obtained 10% detection efficiency for 2.5-MeV neutrons. A special "burst-mode" trigger was set up to gate a LeCroy 9450 digital oscilloscope, which sampled the pulse shape in 2.5-ns bins over a range of 100 μ s. With this arrangement, we added the capability to analyze the short (<50 μ s) bursts reported by LANL, and to perform an energy analysis on the traces to determine if the spectrum is consistent with 2.5-MeV neutrons. These results are not yet conclusive. With more than 200 hours of data acquisition completed, there is no statistically significant difference between the data accumulated while the cell was loaded with deuterium and while the cell was loaded with helium. Roughly half the events in the deuterium sample can be clearly identified as cosmic-ray showers in the lead shielding. Of the remaining events, we see none with more than nine pulses. On the basis of this data, therefore, we can only eliminate the possibility that any bursts of 100 or more neutrons have occurred while the apparatus was operating in this mode. We are currently changing the experiment to achieve sensitivity to 100- μ s bursts with as few as 50 neutrons emitted from the cell. After completing a round of measurements with H-D gas, the upgrade will allow us to set more sensitive limits with D₂. Our efforts will conclude with a search for D-T cold fusion in metal hydrides at high pressure.

Table C-1. Limits on the production of cold fusion neutrons in metal

hydrides at high pressure. P is the pressure of D_2 in the cell, T is the cell temperature. The subscripts i and f indicate values at the beginning and end of the run, the subscripts min and max indicate that the parameter was cycled in this range during the run. The final two columns give the limits on fusion enhancement derived from our data. The "burst" limits apply to the number of neutrons emitted in pulses of less than 100- μ s duration. The continuous production limits constrain the *average* emission rate (neutrons/s) over a 30-minute period. Limits for continuous production over a 15-minute period, for example, are twice as high. Neutron production at the given levels would have increased our count rate by five standard deviations above the level actually observed. For comparison, experimenters at Frascati reported bursts of 2×10^5 neutrons and steady-state production of 5000 neutrons/s. Researchers at LANL report bursts of 30–300 neutrons and steady-state production of a few per minute.

| Sample Type | Notes | P (atm) | T (C) | Hours | Neutron Production Limits | |
|------------------|---|-------------------------|------------------------------------|-------|---------------------------|------------|
| | | | | | Burst | Continuous |
| 25.5 g Va powder | Immediate hydriding | 10 | 24 | 12 | 13,400 | 1200 |
| 47.8 g Ti sponge | Baked under air, 400°C | 10 | $T_i = 300$ | 18 | 1000 | 9.3 |
| | Immediate hydriding | 0 | $T_f = 20$ 20 | 6 | 950 | 9.3 |
| 98 g Ti shavings | No surface preparation. No hydriding. | 12 | $T_{min} = -197$ $T_{max} = 20$ | 80 | 650 | 4.1 |
| | Evacuate and warm. | 0 | $T_i = -197$ $T_f = 20$ | 5 | 650 | 4.1 |
| | Vacuum bake, 30 hr, 400°C. Allow surface hydride, cool before high pressure | 12 | $T_{min} = -197$ $T_{max} = 20$ | 44 | 575 | 3.7 |
| | Evacuate and warm | 0 | $T_i = -197$ $T_f = 20$ | 73 | 550 | 3.7 |
| | Vacuum bake, 30 hr, 380°C Cool before pressure. Partial bulk hydriding | 12 | $T_{min} = -197$ $T_{max} = 20$ | 16 | 460 | 4.1 |
| | Evacuate and warm. | 0 | $T_i = -197$ $T_f = 20$ | 5 | 420 | 4.0 |
| | Cool, pressurize, and warm. Bulk hydriding | $P_i = 12$ $P_f = 9$ | $T_i = -197$ $T_f = 20$ | 14.5 | 500 | 3.7 |
| | Temperature cycle. | 9 | $T_{min} = -197$ $T_{max} = 0$ | 20 | 525 | 3.7 |

Table C-1, Cont.

| Sample Type | Notes | P (atm) | T (C) | Hours | Neutron Production Limits | |
|------------------|---------------------------------------|---------|------------------------------------|-------|---------------------------|------------|
| | | | | | Burst | Continuous |
| | Evacuate and warm | 0 | $T_i = -197$ $T_f = 0$ | 15 | 475 | 3.7 |
| 50 g Ti shavings | Surface oxidation, minimal hydriding. | 50 | $T_{min} = -197$ $T_{max} = 20$ | 92 | | 4.4 |
| | Evacuate and warm. | 0 | $T_i = -197$ $T_f = 20$ | 32 | | 4.4 |
| 5.0 g Pd wire | Unannealed. Minimal hydriding. | 9 | 20 | 10 | 475 | 3.8 |
| | Evacuate. | 0 | 20 | 10 | 500 | 3.8 |
| 5.0 g Pd wire | Annealed, hydriding. | 9 | 20 | 18 | 525 | 3.8 |
| | Evacuate. | 0 | $T_{min} = 20$ $T_{max} = 60$ | 17 | 400 | 4.0 |

Appendix D

Helium and Tritium Analyses

B. Hudson, M. Caffee, B. Ruiz, M. Ruggieri,
R. Nagle, and A. Delucchi
Nuclear Chemistry Division

Appendix D

Helium and Tritium Analyses

We report results for helium, tritium, and gamma-ray activity from four different experiments:

- 1) O-group (Pd metal sheet), M. Ishikawa (See Appendix B.)
- 2) C&MS (Pd wire), Joe Farmer (See Appendix A.)
- 3) Texas A&M (small Pd wire), S. Srinivasan, c/o Joe Farmer
(See Section II, "Summary.")
- 4) University of Utah (Pd wire), c/o John Morrey (PNL) (See Section II.)

Helium was measured for all samples. Tritium in the electrolyte was measured in experiments 1 and 3. Gamma-ray activities were measured in experiments 1 and 4.

Helium Measurements (M. Caffee, B. Hudson, B. Ruiz)

Helium was analyzed using conventional static noble gas mass spectrometry. Two different mass spectrometers were used. The first (MS1) is a Nuclide 6-in.-radius, 60-degree magnetic sector spectrometer with mass resolution of 200. We routinely analyze large gas samples in MS1, and frequently these samples have high levels of helium-3. The second instrument (MSG) is a much newer VG5400 with a 12-in. radius, 90-degree magnetic sector spectrometer with mass resolution of 600. The resolving power of MSG completely separates the mass peaks of helium-3 and HD, and helium-4 and D2. Only air samples were analyzed in MSG before these experiments.

Helium was released by heating the sample in a resistance-heated molybdenum crucible. Chemically reactive gases were removed by exposure to active metal surfaces (getters). We have used combinations of Ti-Zr at 800°C, Ti-Al at 20–450°C, and Cu/CuO at 450°C. The noble gases are separated using activated charcoal. At liquid nitrogen's boiling temperature, activated charcoal collects Ar, Kr, and Xe, leaving only He and Ne in the gas phase. We did not separate He and Ne before analyzing the He.

The mass spectrometer sensitivity was calibrated by analyzing known quantities of air (helium-4 is 5.24 ppm in air). Calibration samples range from 10^{11} to 10^{13} atoms helium-4.

The results are shown in Table D-1.

Table D-1. Helium results.

| Sample | Spectrometer | Sample mass (grams) | Helium-4 (atoms) | Helium-3 (atoms) |
|---|--------------|------------------------|---------------------|---------------------|
| (Experiment 1) | | | | |
| Aliquot 1 | MS1 | 0.24 | <8.e8 | <2.e8 |
| Aliquot 2 | MS1 | 0.17 | <4.e9 | <4.e8 |
| (Experiment 2) | | | | |
| Reference | MS1 | 0.43 | 6.e10 | <2.e10 |
| GC-unheated | MS1 | 0.57 | 5.e10 | <2.e10 |
| D ₂ O cell | MS1 | 1.29 | 2.e11 | <6.e10 |
| (Experiment 3) | | | | |
| Aliquot 1 | MSG | 0.017 | <5.e8 | <3.e5 |
| Aliquot 2 | MSG | 0.018 | <5.e8 | <3.e5 |
| (Experiment 4 data are in but not released by John Morrey of PNL) | | | | |
| Sample A | MS1 | 0.38 | | |
| Sample B | MS1 | 0.38 | | |
| Sample C | MS1 | 0.38 | | |
| Sample D | MS1 | 0.38 | | |
| Sample E | MS1 | 0.38 | | |

Tritium Measurements (M. Ruggieri)

We used low background liquid scintillation counting for all the electrolyte samples analyzed. Our limit of detection for tritium by this method is about 1.0 pCi/ml (2×10^7 atoms/ml).

From each sample, 1.0 ml aliquots were pipetted into tared vials, weighed, and mixed with liquid scintillation counter (LSC) cocktail. These prepared samples (along with standard and background samples) were then counted for 800 minutes. To confirm that tritium was the only beta-emitter, samples were distilled and recounted. The results were unaffected by distillation and confirm that we were only measuring tritium beta decays.

The tritium concentrations of the samples were near values measured for ambient atmospheric HTO so that modest atmospheric exposure would not cause serious contamination. Table D-2 shows the results.

Table D-2. Tritium results.

| Sample | Tritium activity (pCi/g D ₂ O) |
|--------------------------------------|--|
| (Experiment 1) | |
| D ₂ O, lot 118f-3707 | 56.4 |
| LiOD (pre-experiment) | 57.1 |
| D ₂ O exposure blank | 56.4 |
| e3a10 (post-experiment) | 63.4 |
| (Experiment 3) | |
| Fresh LiOD | 37.1 |
| LiOH (60 ma/cm ² 2 days) | <1.4 |
| LiOD (60 ma/cm ² 14 days) | 54.3 |
| "35-MW cell" | 35.7 |

These tritium activities are approximately those of seawater with all H removed, leaving only D₂O and DTO behind.

Gamma-ray Counting Measurements (R. Nagle and A. Delucchi)

We counted all samples from experiments 1 and 4 with a high-efficiency, low-background, GeLi well detector. For all samples (24–100-hr counting time) we have detected no activity above background levels. In particular for ¹⁰⁵Ag ($t_{1/2} = 40$ d), we have seen less than 0.01 dpm activity (less than 1000 atoms now).

The lack of ¹⁰⁵Ag production sets limits on the D+D → p+T fusion reaction. We estimate that for every D+D → p+T, about 10⁻⁷ atoms of ¹⁰⁵Ag should be created by proton capture in the Pd. Thus no more than 10¹⁰ to 10¹¹ D+D → p+T reactions could have occurred, depending on when the experiment took place.

Appendix E

A Study of "Cold Fusion" in Deuterated Titanium Subjected to High Current Densities

R.B. Campbell and L.J. Perkins

Appendix E

A Study of "Cold Fusion" in Deuterated Tritium Subjected to High Current Densities

Introduction

The original announcement of the observation of "cold fusion" phenomenon in electrochemical cells by Fleischmann and Pons [1] (FP) sent many researchers around the world to their laboratories to attempt to reproduce the results. The original reports from FP indicated that about four times as much power was liberated from "fusion" reactions as was consumed by the cell. The excess enthalpy generation was claimed to increase with the applied current density, as well as the sample volume [1]. Large extrapolations in " $Q = P_{fus}/P_{input}$ " were made for larger samples at higher current density. The large Q value, as well as the dependence on current density, motivated us to embark on the present study. Based on the FP results, the excess heat should be easily observed, and should therefore be measurable by an apparatus which has a relatively low sensitivity. Other workers [2] have demonstrated that the excess heat, if observed at all, is substantially smaller than that reported by FP, and fairly sensitive calorimetry is necessary to see the effect. Therefore, the results we present here establish that the excess heat released is below a certain level. Based on our experiments, the excess heat was zero, within the estimated accuracy of our apparatus.

We adopt the resistive circuit approach with deuterated titanium instead of the electrolytic cell with a palladium cathode for several reasons.

First and foremost, the resistive circuit isolates the effect of current and current density from other effects associated with the electrolysis process. Our apparatus tests the possibility that the role of high current density in the FP experiments is to create such non-equilibrium states as strong pinching due to current micro-channeling in the metallic lattice. This strong pinching, in turn, could reduce the deuteron-deuteron separation sufficiently to cause significant fusion. A second reason for the use of the resistive circuit is that the ability to pass large currents (≈ 50 A) through massive samples (≈ 30 g) is quite easy by using a resistive circuit driven by a constant current power supply. By using a single circuit consisting of a deuterated sample and a hydrogen control sample in series, temperature differences can be measured and related directly to the excess enthalpy generated in the deuterated sample. Estimates of excess enthalpy generation as a fraction of the ohmic dissipation are possible by comparing the temperatures of the active sample and the control sample relative to the ambient temperature. The accuracy of such a scheme is limited by our ability to create identical electrical resistances and heat-transfer environments for the active element and the control. We insure that the electrical resistances are the same by direct measurement, and we equalize the heat-transfer environment by measuring temperature differences between two identical samples of elemental titanium substituted in the circuit. Based on these calibrations, we believe that the error in our apparatus is on the order of 10%, about the same as the upper bound of the fractional excess enthalpy we infer from the loaded sample temperature differences.

We use titanium instead of palladium for two reasons. First, the titanium can be loaded to concentrations of up to 2:1 D:Ti, substantially larger than that attainable with palladium. Because the titanium becomes very

brittle at high loadings, we limit our loading to approximately 1:1, on the same order as the rumored loading of the FP electrodes [2] of 1.1:1 (D:Pd) under the influence of a strong electrochemical overpotential. The second reason for using titanium is that the titanium and hydrogen isotope form a stable compound in the temperature ranges at which we operate the resistive experiments. Our operating temperature range is from room temperature to about 100°C. Palladium containing hydrogen isotopes, on the other hand, is observed to outgas readily at these temperatures, and in fact is a catalyst for the exothermic recombination of hydrogen and oxygen into (heavy) water vapor. Therefore, the use of titanium eliminates one possible chemical explanation for the excess heat observed by FP.

Deuterated and hydrogenated titanium samples are readily available from washer guns used on the mirror device 2XIIB [3]. These rings of titanium are annealed at high temperature (1100°C) for several hours at high vacuum. D₂ or H₂ gas introduced at these temperatures is easily absorbed in about an hour into the sample. Consequently, annealing of the material occurs naturally as a part of the deuterating process. Annealing is claimed to be an important element in the cold fusion process [2].

Experimental Apparatus

Figure E-1 shows the experimental setup which we have constructed to search for cold fusion. The circuit consists of two washers loaded with either hydrogen or deuterium, connected in series with #6 copper welding cable. Care was taken to be sure the lengths of wire connecting each of the samples were kept the same, in order to keep the thermal mass and electrical resistance of each sample unit the same. The samples are isolated thermally from each other, and the power supply by three heat sinks maintained at

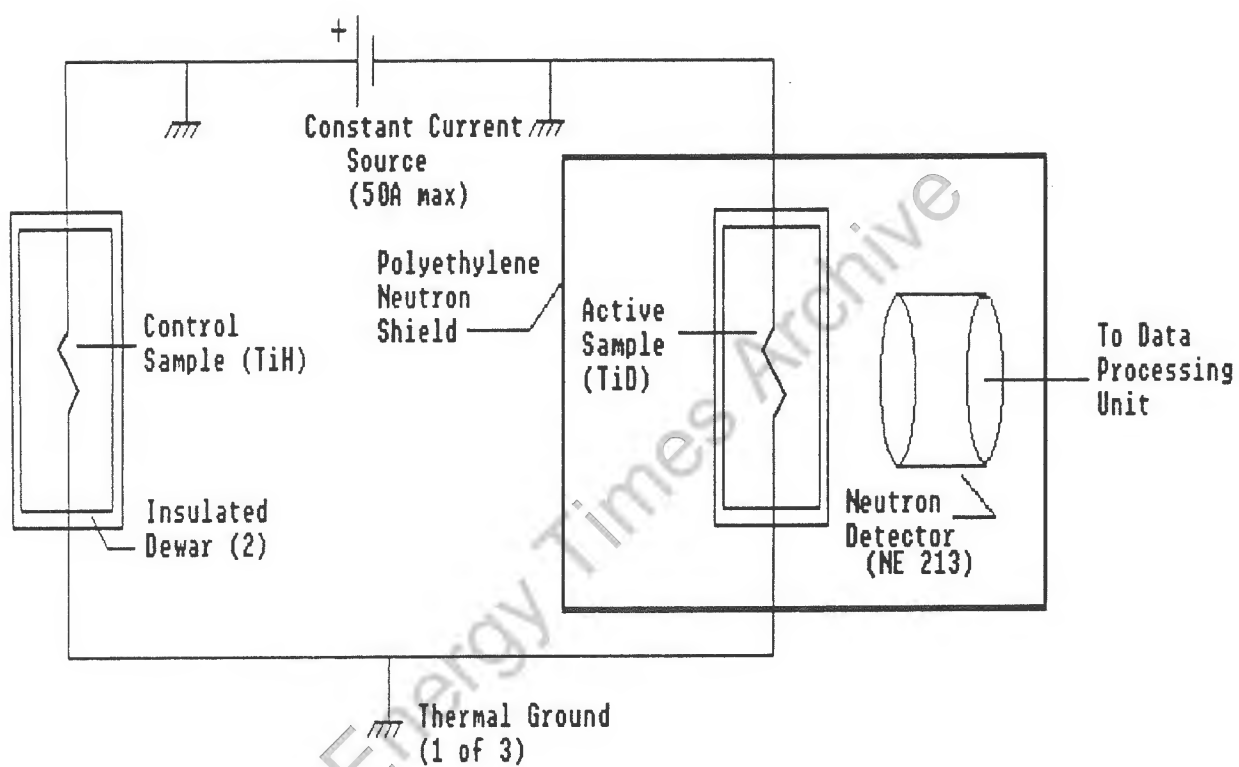


Figure E-1. Resistive circuit used for cold fusion investigations.

room temperature by forced convection. The purpose of these heat sinks is to eliminate conduction heat transfer between the samples and the power supply. Conduction heat transfer would modify the temperatures between the sample and the control. These sinks are denoted by the ground (thermal *not* electrical) symbols on the diagram. At each of the sinks, the conduction heat transfer into the junction is removed by forced convection, thereby eliminating thermal crosstalk between the two samples. Type "K" thermocouples are attached to the samples and each of the heat sinks to monitor the temperature differences of all the elements during the experiment. The accuracy of these thermocouples is about $\pm 0.1^{\circ}\text{C}$. The temperature data are taken and recorded periodically with a strip chart-type data logger.

The neutron data is compiled with a NE213 liquid scintillator based spectrometer, with gamma counts eliminated using pulse-shape discrimination. The pulse height spectrum data were processed and stored automatically by a Toshiba T-1100+ microcomputer. A more detailed description of the neutron spectrometer apparatus can be found in Ref. 4. The deuterated sample to be diagnosed for neutron emissions is housed in a polyethylene "igloo" to reduce the neutron background. The average thickness of the igloo walls is about 10 cm, and we estimate the background counts are reduced by about a factor of three by this shielding. The distance from the sample to the detector face is such that the subtended solid angle is about $0.02 \times (4\pi)$.

The igloo tends to change the convective heat transfer environment of the deuterated sample, so each of the samples are housed in a vacuum dewar and the lids and outer walls of the dewar are heavily insulated. This step,

combined with the careful measurement of lead-wire lengths, is important to make the bulk heat transfer coefficients of the two samples the same. This heat transfer coefficient, along with the temperature difference between the active sample and the control, are used to determine the upper limit of the enthalpy production rate due to any "fusion" process. Based on calibrations with blank titanium rings, we estimate we can make the resistances and heat transfer coefficients the same to within 10%.

Experimental Procedure

Before we begin an experimental run to look for the effects of cold fusion, the detector's energy scale is calibrated with a Bi^{207} gamma source and then a background neutron count is taken. The count time is either 18 or 19 hours, depending on the case considered. The active run with the sample in place typically begins within 3 hours of the completion of this background run, with the same counting time.

The circuit is then balanced between the hydrogenated control and the deuterated active sample with respect to electrical resistance, thermal mass, and heat transfer geometry. The samples are pre-loaded with hydrogen isotopes to obtain the same electrical resistances. For the loading densities we employ, about 0.9(D,H):1(Ti), the electrical resistance is about twice that of elemental titanium. Although full stoichiometric loading [i.e., 2(D,H):1(Ti)] of these samples is possible, they become prone to fracture due to hydrogen embrittlement above loading densities about 1:1; thus our limit of 0.9:1. The loading of 0.9:1 in our samples is above the room temperature stoichiometry of $\text{PdD}_{0.7}$, and approximately equal to the stoichiometry of $\text{PdD}_{1.1}$ which has been rumored to exist in the FP electrodes [2] under the effects of a strong overpotential. The most difficult step in this balancing process is the

equalizing of the contact resistances between the copper lugs attached to the welding cable and the samples. The contact surfaces are polished with emery paper and degreased with Freon. The samples cannot be welded because the hydrogen would be evolved from the metal during heating. We therefore attach the lug and sample with a C-clamp. Typical contact resistances we encounter are on the order of 1 m Ω per sample. The heat transfer conditions for the two samples is equalized by the careful insulation of the both the dewars and the cables exiting them. We establish when the heat transfer environments are comparable in each case by monitoring the temperatures of the two samples relative to the heat sinks. Typically, before we begin a run with current applied, the temperatures of the two samples are within 0.5° of each other, and a degree or two above the convectively cooled thermal ground.

When the current is turned on, we monitor the rise of the sample temperatures as well as the temperatures of the heat sinks. We also monitor the resistance of the samples to account for the change in resistivity as the sample rises in temperature. The temperatures of the samples exceed the sink temperature by 20–40°C; the exact value depends on the applied current. For the cases examined, the temperatures of the samples track each other rather closely, suggesting that the total volumetric heating ($I^2R + P_{fus}$) is quite similar. Since no excess enthalpy production is expected in the hydrogen control sample, the small temperature difference between the two samples can be used directly to determine an upper bound on P_{fus} .

When the neutron counting has been completed, the current is turned off and the temperature is allowed to decay. This decay time can also be used to estimate the overall heat transfer coefficient.

4. Results and Analysis

4.1 Neutron Measurements

The pulse height spectrum from our neutron spectrometer is shown in Fig. E-2 for three cases. The raw counts during an 18-hour run are shown on the vertical axis, and the recoil proton energy on the horizontal axis. Because of the relatively poor statistics in these neutron counts, we do not unfold this spectrum to obtain an incident neutron spectrum. Shown in this figure are three separate conditions during which we took data.

The first condition is without any deuterated titanium present. These background counts are the average of the results of three 18-hour runs. The averaging allows us to improve statistics and to account for, in a simple way, the expected natural variation of the neutron background on a day-to-day basis. Data are also shown for two current levels, one at 20 A, the other at 30 A. These two currents correspond to current densities of 30 and 46 A/cm², respectively. There appear to be no statistically significant counts above background for either current level, within the error bars shown. Notice that some weak structure* in the proton recoil spectrum, suggestive of a neutron peak, exists in the range of 2–3 MeV, for each set of data. We believe this phenomenon is due to the inability of the pulse-shape discrimination to eliminate completely the background gamma counts. This is a problem well recognized in the neutron measurement community, and is particularly problematic at the very low levels we are trying to measure [5]. One possible

* A step in the proton recoil spectrum can indicate the presence of neutrons at an energy where the step occurs.

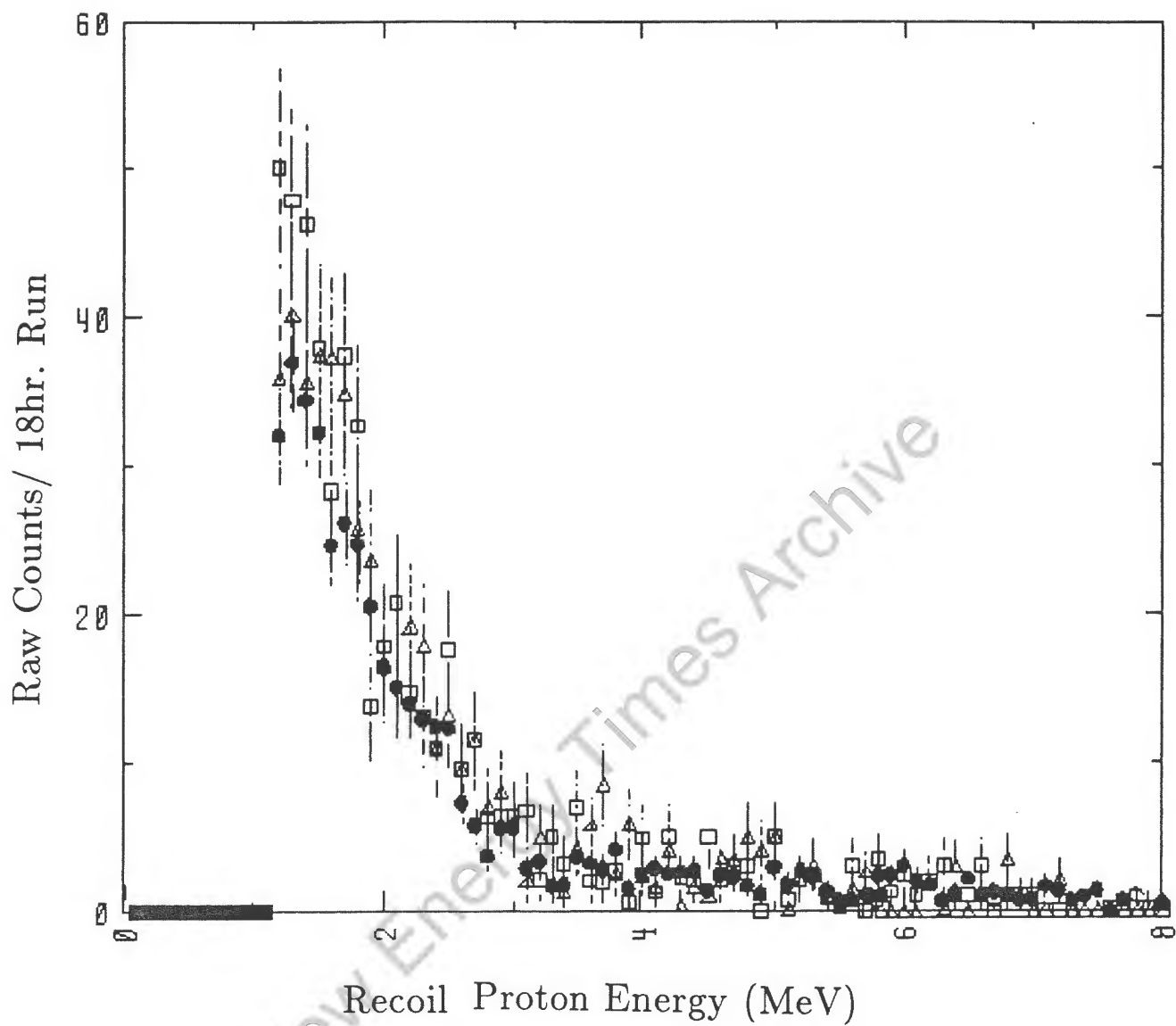


Figure E-2. Proton recoil pulse height spectrum. The dots are an average of three 18-hour background runs. The triangles and squares are the spectrum obtained at current densities of 30 and 46 A/cm², respectively.

way to correct this deficiency is to add a coincidence measurement of gamma counts using a NaI detector.

4.2 Excess Heat Measurement

Figure E-3 shows the time dependence of the temperatures in the apparatus as the current is first turned on to 20 A, and then when it is raised to 30 A after about 20 hours of operation. The temperatures of each of the samples, as well as the average temperature of the three heat sink "grounds," are shown. Notice that the temperatures of the two samples track each other fairly well, and both can rise well above the temperature of the heat sinks. The exponential rise times, τ , of both of the samples from the zero current condition are between 80 and 90 minutes. The temperatures of the heat sinks remain quite steady at their $I = 0$ values for the duration of the experiment.

The determination of excess rate of enthalpy production is facilitated by considering a simple bulk energy balance:

$$M_{bulk}C_{p,bulk}\frac{dT_{bulk}}{dt} \approx P(t) - h_{eff}A_{eff}[T_{bulk}(t) - T_{\infty}] \quad (1)$$

In Eq. (1), P is the total power release in the sample, and T_{bulk} is the bulk temperature of the sample, C-clamp, lugs, and a small length of the copper leads. Good thermal conductivity within the titanium sample and connecting hardware suggests that a uniform temperature is a reasonable approximation. The temperature T_{∞} is the ambient temperature. The product of the overall heat transfer coefficient, h_{eff} , and effective heat transfer area, A_{eff} , is an experimentally determined quantity. This term includes the effect of both conduction through the leads and natural convection to the interior

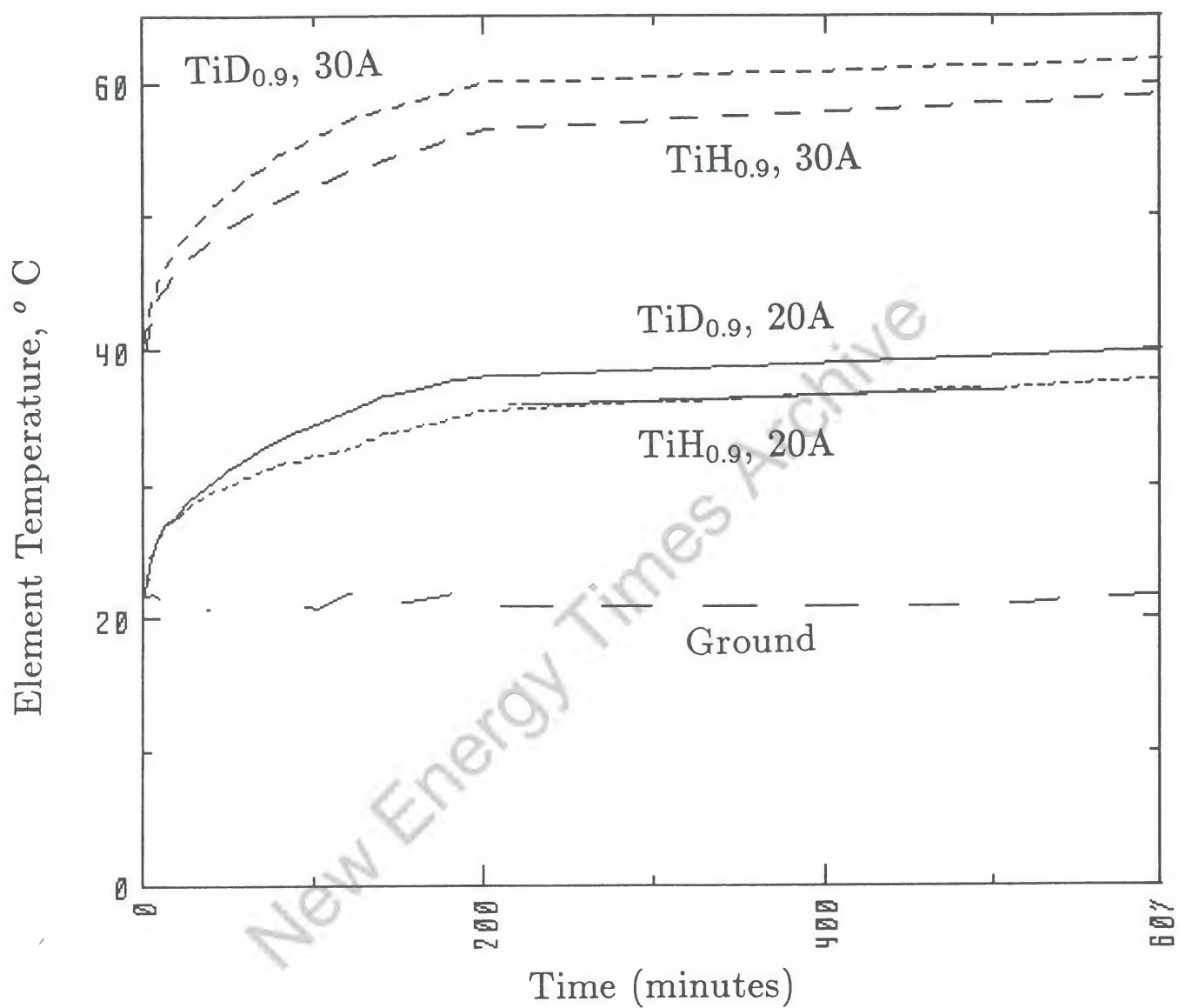


Figure E-3. Time history of the temperatures of samples and thermal ground for 20-A and 30-A currents.

of the vacuum dewar. Since the insulation provided by the dewar is quite good, we expect the major heat loss to be conduction through the leads. This suggests that it is reasonable to take T_{∞} in Eq. (1) as the heat sink temperature. The mass of the C-clamp, lugs, and leads within the dewar are important to include when computing the effective thermal mass, M_{bulk} , and when calculating the heat transfer coefficient from the time constant of the temperature rise, τ .

It is possible to use Eq. (1) directly to yield an estimate of the temperature rise of the sample due to ohmic heating only. However, difficulties associated with the assignment of an effective heat transfer mass and bulk heat capacity usually make this calculation inaccurate. A better approach, adopted here, is to simply look at the steady-state temperature differences between the active sample and the control sample. For samples with the same heat transfer geometry (i.e., same $h_{eff} A_{eff}$), the steady state $T_{bulk} - T_{\infty}$ values will be in the same ratio as the enthalpy production rates in each sample. The steady state solution of Eq. (1) is

$$T_{bulk} - T_{\infty} = (P_{\Omega} + P_{fus}) / (h_{eff} A_{eff}) \quad (2)$$

where P_{Ω} is the joule heating power.

By taking the ratio of $T_{bulk} - T_{\infty}$ from each sample, we can estimate the upper limit of the excess rate of enthalpy production. For the 20-A case, the excess rate of enthalpy production does not exceed 0.085 W, or 11% of the ohmic dissipation. For the 30-A case, P_{fus} does not exceed 0.14 W, or 8.5% of P_{Ω} . By our calibration of the circuit with titanium blanks, we know that the heat transfer coefficients of the two samples can differ by about 10%. This

suggests that the "excess enthalpy" we have calculated above is probably a manifestation of the differences between the values of $h_{eff} A_{eff}$. It is clear from these measurements that any fusion power production is far below a break-even level, even at very high current densities.

We now examine what the FP scaling of the excess enthalpy production with current density and volume would predict. Ref. 1 claims that a sample subjected to a current density of 0.064 A/cm^2 and a volume of 0.078 cm^3 has an excess volumetric heating of 1.01 W/cm^3 . To be conservative in our extrapolations, we ignore the claimed linear dependence on volume of the sample, and we focus attention on the roughly linear dependence on current density. This extrapolation results in an excess volumetric heating of almost 500 W/cm^3 for the 20-A case. The sample volume is about 6.5 cm^3 , resulting in a total enthalpy production rate of about 3 kW. This amount of power, if present, would make the deuterated sample red hot, and make thermal radiation the dominant heat loss mechanism. These high temperatures are not observed in our experiments.

5. Conclusions

Our experiments show that there is no significant neutron emission or excess enthalpy production in relatively massive samples of deuterated titanium $\text{TiD}_{0.9}$ subjected to high current densities of up to 50 A/cm^2 . If we assume that chemically stable $\text{TiD}_{0.9}$ is fundamentally the same as $\text{PdD}_{\approx 1}$, with respect to bringing deuterons close enough together within the lattice structure to cause fusion, our results suggest that current density and volume do *not* play a direct role in the unknown process producing excess heat reported by Fleischmann and Pons.

Acknowledgments

We would like to acknowledge the kind assistance of several individuals in obtaining materials and equipment on such short notice for use in our experiment: J.E. Bowman, M.R. Chaplin, M. Malonowski, W.E. Nexsen, Jr., L.T. Summers, and J.H. Thorngate.

References

- [1] Martin Fleischmann, B. Stanley Pons, and Marvin Hawkins. "Electrochemically Induced Nuclear Fusion of Deuterium." *J. Electroanal. Chem.*, **261**, 301–8, (1989).
- [2] Los Alamos National Laboratory. Workshop on Cold Fusion Phenomenon. Santa Fe, New Mexico, May 1989.
- [3] V.A. Finlayson. *Procedure for Deuterating Titanium*. Report UCID-15624, Lawrence Livermore National Laboratory, March 7, 1970.
- [4] John H. Thorngate. *Using the Transportable, Computer-Operated Liquid-Scintillator Fast-Neutron Spectrometer System*. Report UCID-21548, Lawrence Livermore National Laboratory, November 1, 1988.
- [5] M. Gai et al. "Upper Limits on Emission Rates of Neutrons and Gamma-Rays from Cold Fusion in Deuterated Metals." Yale-Brookhaven Collaboration, Yale-3074-1025, Yale University, May 20, 1989. Submitted to *Nature*.

Appendix F

Surface Analysis of Palladium Wire

A. Connor and C. Colmenares

Appendix F

Surface Analysis of Palladium Wire

Introduction

Surface analyses of Pd wire used in two different electrolytic cell experiments were performed. The first wire was from the LLNL first matched-cell experiment (Appendix A), while the second was from wire received from Texas A&M. That material was used in a cell where excess heat was reported.

1. Texas A&M Material

Analysis Requested

We were asked to determine the composition of the black material on the surface of the palladium wire, looking especially for lithium, sulfur, and arsenic.

Analysis Procedure

The sample was analyzed on the Perkin-Elmer 600 Multiprobe using Auger electron spectroscopy (AES) and secondary ion mass spectroscopy (SIMS), and on the Perkin-Elmer 5400 ESCA system using x-ray photoelectron spectroscopy (XPS).

After verifying that the wire being analyzed was indeed made of palladium, an AES survey of the black material was taken to see what elements were present. Scans of the individual elements were then taken to determine concentrations. Next, the sample was sputtered for 1 minute at $\sim 200 \text{ \AA/min.}$ using 4 kV Ar^+ ions, and then was surveyed again. Positive

and negative SIMS surveys were taken next to see what trace contaminants might be present.

The sample was removed from vacuum and transferred to the ESCA system for XPS analysis. The black area was surveyed to see what elements were present. Because there was reason to believe that the analysis point was not perfectly aligned, no further data were taken; if desired, it can be pursued after the system has been realigned.

Results

Carbon, chlorine, calcium, oxygen, and iron were found on the black material in the initial AES survey of the as-received surface. A small amount of silicon may also have been present. Concentrations are given in Table F-1.

One minute of sputtering removed nearly all of the carbon. At that point, chlorine, calcium, palladium, nitrogen, oxygen, iron, and copper were detected. Two other peaks were tentatively identified as platinum and cerium. Concentrations excluding the two "uncertain" peaks are given in Table F-1.

The positive SIMS survey showed the presence of H, Li, B, N, O, Na, Al, K, Ca, Ti, Cr, Fe, Cu, As, Mo, Si, and possibly Mg and Ba. In addition, visible on the negative SIMS survey were F and Cl. A number of higher-amu peaks were also present which are molecular fragments rather than single

Table F-1. Concentrations on black material on palladium wire, determined by AES (atomic percent).

| | Ca | O | C | Fe | Cl | Pd | N | Cu |
|------------------|------|------|------|------|-----|-----|-----|-----|
| As received | 12.3 | 38.7 | 41.2 | 6.6 | 0.9 | — | — | — |
| 1-min sputtering | 17.4 | 33.9 | — | 32.2 | 0.8 | 5.3 | 2.4 | 8.0 |

atoms, and most of these were not identified. SIMS is a completely qualitative technique, and thus elemental concentrations cannot be extracted from the data.

The XPS data were taken with the intention that some oxidation states might be determined, but because there was some uncertainty about the accuracy of alignment (which might result in detection of elements from other areas on the sample or on the mount), and because the signal was very low, only a broad survey was taken to see what elements might be present. Elements seen on the surface were iron, fluorine, oxygen, molybdenum (possibly from the sample mount), calcium, carbon, silicon, and platinum. No concentrations were determined. If oxidation-state information is needed, more data may be taken after realignment of the instrument.

Of the elements of particular interest, only a trace of arsenic was seen by SIMS, and it was not detected by the other techniques. Small amounts of sulfur could not be definitely detected by SIMS due to interference with the O₂ peak, but as no sulfur was seen on either the AES or XPS analyses of the black material, it can be definitely stated that no more than 0.5% was present. Both AES and XPS are very insensitive to lithium, making small amounts difficult to detect, but the lithium peak seen on the SIMS survey is well above the normal background for a clean sample.

Copies of some of the data are attached as Figs. F-1 through F-4.

2. LLNL Matched-Cell Wire

Analysis Requested

We were asked to determine the presence and depth of penetration of contaminants, especially lithium, on the surface of the two electrodes.

Analysis Procedure

Analysis was performed on the Perkin-Elmer 600 Multiprobe using Auger electron spectroscopy (AES) and secondary ion mass spectroscopy (SIMS), and on the Perkin-Elmer 5400 ESCA system using x-ray photoelectron spectroscopy (XPS).

The sample was first surveyed using AES to see what elements were present on the surface and estimate concentrations. The sample was then sputtered for 1 minute at $\sim 35 \text{ \AA/min}$ using 4 kV Ar^+ ion bombardment to remove atmospheric contamination, and was surveyed again.

Next, the surface was surveyed using SIMS to see what elements could be detected. A depth profile was then taken at a sputter rate of 100 \AA/min to try to estimate the depth of contaminant penetration. Another survey was then taken at the end of the profile.

The sample was then transferred to the ESCA system. It was surveyed over a $600\text{-}\mu\text{m}^2$ area, again to see what elements could be detected and to estimate concentrations. It was sputtered for 2 minutes at 30 \AA/min to remove atmospheric contamination, and then was surveyed again.

Sputter rates were calibrated on a $1000\text{-}\text{\AA}$ layer of Ta_2O_5 on Ta.

Results

The following elements were detected by AES: silicon, sulfur, chlorine, carbon, calcium, palladium, oxygen, iron, and possibly copper and magnesium. Concentrations determined on the surface are given in Table F-2. SIMS detected the presence of hydrogen, lithium, carbon, sodium, aluminum, potassium, calcium, iron, palladium, and possibly titanium, chromium, and copper. XPS showed iron, oxygen, calcium, palladium, carbon, silicon, and a trace of aluminum; concentrations are given

Table F-2. Concentrations on Pd electrode determined by AES (atomic percent).

| Si | Cl | C | Ca | Pd | O | Fe | Mg |
|-----|-----|------|-----|-----|------|-----|-----|
| 5.2 | 0.6 | 41.0 | 8.8 | 1.4 | 33.3 | 5.2 | 4.8 |

in Table F-3. Differences in the concentrations between the XPS and AES data are probably due to several factors, including variations in the sample surface, especially carbon coverage from atmosphere, and differences in sensitivity to the elements in Table F-3.

Both AES and XPS have peak interferences which make it impossible to detect lithium. SIMS did show that lithium is present, but because this technique is purely qualitative, no concentrations could be determined. Also, SIMS showed the lithium to be greatly enriched in the amu 6 isotope; normal isotopic abundances are 7.52% (amu 6) and 92.5% (amu 7); the SIMS data showed the amu 6 peak to be 2–10 times that of the amu 7 peak.

The sodium and potassium signals on the SIMS data are normal for most samples; the sensitivity of SIMS to these elements is so high and they

Table F-3. Concentrations on Pd electrode, determined by XPS (atomic percent).

| | Fe | O | Ca | Pd | C | Si |
|------------------|-----|------|-----|-----|------|-----|
| As received | 0.8 | 38.6 | 2.5 | 1.1 | 52.8 | 4.3 |
| 2-min sputtering | 2.6 | 44.4 | 3.6 | 2.1 | 39.1 | 8.2 |

are so prevalent that they are always seen in all but the purest of samples. Other elements detected on the SIMS spectrum, however, are at contaminant levels.

Because of the curvature and roughness of the sample surface, no accurate depth determinations could be made, and it is not known how far into the sample the contaminants extended. The SIMS depth profile (Fig. F-1) shows a sharp decrease in the Ca, Li, Al, and Fe signals in the first two minutes of sputtering; this is primarily due to the removal of surface oxygen, which enhances the signal of other elements, rather than necessarily to a decrease in concentrations. Shadowing of the ion beam due to the rough, grooved surface of the electrode is probably causing the continued gradual decrease in signals to be slower than the actual change of concentration with depth. The latter problem also exists with both AES and XPS attempted depth profiles; thus no conclusions about contaminant penetration could be drawn from the data.



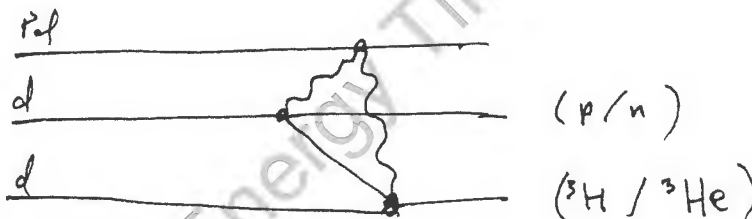
UNITED STATES DEPARTMENT OF COMMERCE
National Institute of Standards and Technology
[formerly National Bureau of Standards]
Gaithersburg, Maryland 20899

September 5, 1989

Dr. John R. Huizenga
Co-Chairman, Cold Fusion Panel
Energy Research Advisory Board
United States Department of Energy
1000 Independence Avenue, S.W.
Washington, DC 20585

In response to your letter of July 20, 1989, I am providing you with a short summary of my past and present research on cold fusion.

1. Past: I demonstrated that a mechanism exists within the framework of standard Schrödinger quantum mechanics which can lead to the observed reaction rates.
2. Present: In collaboration with V. Belyaev I am computing the reaction $d + d \rightarrow p + {}^3\text{H}$ and $d + d \rightarrow n + {}^3\text{He}$ in terms of a second order process. The reaction graph which we are investigating is shown, below. Note the loop in the graph. This, in fact, is to my knowledge the first case where a higher order process dominates overwhelmingly over the first order process.



Sincerely yours,

Michael Danos
Center for Radiation Research
Nuclear Physics Group

Los Alamos

Los Alamos National Laboratory
Los Alamos, New Mexico 87545

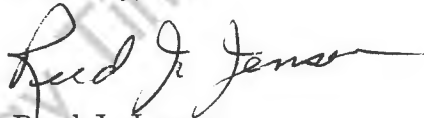
DATE: September 13, 1989
IN REPLY REFER TO: ADR:89-409
MAIL STOP: A114
TELEPHONE: (505) 667-1233
(FTS) 843-1233

Dr. John R. Huizenga
Co-Chairman, Cold Fusion Panel
Energy Research Advisory Board
to the Department of Energy
1000 Independence Avenue, S.W.
Washington, D.C. 20585

Dear Dr. Huizenga:

Please find the enclosed report on cold fusion research at Los Alamos. This report is being provided in accordance with your July 13, 1989, request. We hope it will be useful in your work, and we look forward to seeing your assessment of this subject.

Sincerely,



Reed J. Jensen
Deputy Associate Director
for Research

RJJ:slg

Enc. a/s

Cy: R. Gajewski, ER-16, G-347/GTN
S. S. Hecker, DIR/A100
R. J. Jensen, ADR/A114
C. J. Orth, INC-11/J514
CRM-4/A150 (2)
ADR File

RESULTS OF COLD FUSION RESEARCH AT LOS ALAMOS NATIONAL LABORATORY

Prepared September 11, 1989, for the Cold Fusion Panel,
Energy Research Advisory Board to the U. S. Department of Energy

A broad program of experimental and theoretical cold-fusion research is currently being pursued at Los Alamos. Shortly after Fleischmann and Pons announced their claimed observation of cold fusion in simple electrochemical cells, Los Alamos staff members set out to confirm the Utah results. Electrochemical cells with many different electrolyte and cathode parameters and with nuclear radiation monitoring were put into operation, and the frustration began—there was no evidence of excess heat or fusion products. When it became abundantly clear that cold fusion would be far more difficult (if not impossible) to attain than we were led to believe, the Los Alamos experimental effort settled down to systematic studies of three aspects of cold-fusion phenomena: electrochemical cells, high-pressure deuterium-metal systems, and solid-state Si-Pd cells.

Los Alamos theorists also have investigated several aspects of cold-fusion phenomena. These include reaction rates at very low energies, deuterium-metal cracking phenomena, Heitler-London and James-Coolidge electronic-wave functions for the deuterium molecule in the limit of electron coincidence between the atoms, atomic scale resonance phenomena, the location of deuterons in metal lattices, and electronic screening.

Despite the frustration from the non-reproducibility of experimental results from all aspects of cold-fusion phenomena, Los Alamos researchers continue to work very hard to resolve the controversy over whether cold fusion is a reality or not. The prospect of producing tritium (T) by such a simple technique is too important for us to abandon this research before examining all avenues in an objective and systematic manner.

ELECTROCHEMICAL CELLS

Systematic Study of Cell Parameters

Two investigators have been simultaneously operating up to 22 electrochemical cells with various electrode materials and charging parameters. In the early

going, considerable effort was directed at increasing the D/Pd ratio by alloying and by surface coating techniques. At first the cells were monitored with neutron counters, but as reports of tritium buildup without detectable neutron emission came in from other laboratories, the electrolytes were assayed for tritium. At the end of two experiments (Runs 29 and 30), the electrolytes from the (Pt anode/sulfide-coated Pd cathode) cells both showed about a sixty-fold increase in their tritium content over the concentration of the stock solutions of electrolyte. However, the electrolytes were not assayed in the cells prior to charging, so contamination cannot be ruled out despite the fact that precautions were taken to avoid this possibility. To date, 70 cells have been studied. Except for two special cases, the cells are now fitted with D₂-O₂ recombiners. The special cases are Bockris clone cells that are too small to hold a recombiner. The Los Alamos researchers went to Texas A&M University and traded systems (cells, electrodes, electrolytes, D₂O, rubber stoppers, syringes, and connecting wires) with the Bockris and Martin teams who claim their Ni anode/Pd cathode cells are producing tritium and heat. According to the Texas A&M account, the cells are charged at 50 to 60 mA/cm² for two weeks, and then the current is increased by an order of magnitude to produce significant amounts of tritium within 1 to 21 days. The two clones at Los Alamos are now beginning their third week of high-current operation with no tritium buildup. Each day, all 22 cells are monitored for tritium buildup. If an excess is detected, the indicated cell(s) will be placed alternatively in a high-efficiency neutron counter or before a high-resolution x-ray detector.

A summary of the 70 cells that have been studied to date is given in Table 1. All cells except BB, BM and #70 used 0.2 N LiOD. The three exceptions used 0.1 N LiOD. Total currents ranged from 40 to 1000 mA.

When this work was started, emphasis was placed on determining the D/Pd ratio as a function of charging time. Various electrolytic poisons and surface treatments were investigated to determine their effect on the charging rate and D/Pd ratio. The plug and socket arrangement within the cell, used to facilitate weighing the Pd cathode, caused Cu, Zn, and Pb to be dissolved and deposited on the Pd. Application of Torr Seal to the plug and lead reduced this impurity problem, but the epoxy was found to absorb deuterium, thus adding to the apparent D/Pd ratio. A later design eliminated both problems, but by then the average D/Pd ratio was believed to be relatively unimportant. The newer, more reliable data are also shown in Table 1. The current cell design emphasizes the growth of surface dendrites containing various impurities and the collection of the electrolyzed deuterium gas as D₂O using a recombiner.

Attempts are currently being made to recreate the conditions that have given tritium buildup observed earlier in this work and reported at Texas A&M University and by Glenn Schoessow at the University of Florida.

There is no effort to measure excess heat, except by simple thermometry. However, promising cell configurations from this work are then adopted by another Los Alamos team doing high sensitivity calorimetry. Several Pd + Li alloy cathodes also have been prepared for investigators at Sandia National Laboratories (Albuquerque) and at Texas A&M University.

Calorimetry of Electrochemical Cells

At the Santa Fe Workshop on Cold Fusion Phenomena the importance of careful, closed-system calorimetry was stressed. One team at Los Alamos has constructed a calorimeter that can detect a one-percent change in the ratio of heat output to heat input of an electrolysis cell. The cell is fitted with a Pt catalyst D_2 - O_2 recombiner, a feature that reduces the uncertainty in accounting for escaping D_2 and O_2 , and the uncertainty in tritium balance from differences in D and T volatilities. Neutron and gamma-ray detectors constantly monitor the system, although they are in poor geometry because of the calorimeter's size. Small aliquots of electrolyte can be removed for tritium assay if heat generation is observed. Should any signal of fusion occur, the cell can be quickly placed in or before high-efficiency nuclear radiation detectors.

Thus far, two experiments have been performed. The first involved a Pt anode/cast, 99.8% purity, 2-mm diameter by 5-cm long Pd cathode/0.1 M LiOD cell. It was operated for two weeks at 50 mA/cm² without generation of heat or tritium. The second, currently in operation, involves a Pt anode/2-mm diameter by 5-cm long Pd-Li (Li/Pd ~0.04) cathode/0.1 M LiOD cell. This unit was charged for two weeks at 50 mA/cm², and the current has just been increased to 500 mA/cm². The intent is to operate the cell at this current density for at least three weeks. Thus far, no heat generation or tritium buildup has been detected.

HIGH PRESSURE GAS-METAL SYSTEMS

These studies involve the use of high-efficiency neutron counting of pressurized gas containers. Generally, the containers are loaded with 25 to 100 grams of Ti or Ti-alloy lathe turnings that are exposed to high pressures of D_2 gas, and then are repeatedly cycled in the neutron well counters between liquid nitrogen and room temperature. On rare occasions, small bursts of neutrons (up to about 100 source neutrons during a 50 to 100 μ sec window) have been observed. Control experiments with hydrogen gas have not produced such bursts. Because of the non-reproducibility of these experiments, the hydrogen control measurements will continue. Thus far, Ti-662 alloy (6% Al, 6% V, and 2% Sn) has been more likely to produce neutrons than Ti metal or Ti-64 alloy (6% Al and 4% V). The neutron counters are of the central well or of the channel configuration, polyethylene moderated, with ^3He -filled neutron detector tubes. Efficiencies for ^{252}Cf spontaneous fission neutrons range from 20 to 33%. Three units have two concentric rings of

tubes and one unit contains three rings, designed to provide neutron energy resolution. In most of these measurements acoustic sensors are placed on the pressure vessels to detect cracking. Earlier, the fracture or cracking mechanism was considered a likely candidate to provide the accelerating potentials for fusion reactions. The acoustic sensors indicate otherwise; correlations between cracking noise and neutron bursts have not been observed. In measurements with the neutron counter containing three rings of detector tubes, a pressurized gas container was converted to an ionization detector so that ionization and neutron emission could be measured simultaneously, on the consideration that ionization events and electron emission should be far more intense than neutron emission in the cracking process. Several ionization events from small (1 g) Ti foils have been observed, but not in coincidence with neutrons. The cracking mechanism for neutron production, although unlikely, will be further investigated with insulators (SiO_2) in the place of Ti and its alloys.

The conditions and results for most of the pressurized gas/metal experiments are given in Table 2.

If conditions can be found that give reproducible neutron production, the use of DT gas will help provide an estimate of the reaction temperature. The ratio of 14-MeV neutrons from the D-T reaction to 2.5-MeV neutrons from the D-D reaction contains temperature information. If local hot fusion is occurring, D-T gas should yield at least 10 times more neutrons than D-D gas because of the higher probability for the D-T reaction (see Figs. 2 and 3 and the discussion under THEORETICAL ACTIVITIES). Conversely, if the reactions are "cold," metal lattice vibrational energies are very low (<1 eV) and the D-D reaction rate should be greater than the D-T rate.

SOLID STATE Si-Pd CELLS

The motivation for the following solid-state cell design (Fig. 1) was to create a metal-insulator semiconductor junction where a non-equilibrium condition could be produced either by electron injection or by diffusion of deuterium ions. The small cells are constructed of alternating wafers of Pd powder and of slightly oxidized Si powder pressed into a monolithic, gas permeable pellet that is exposed to D^2 gas at 110 psia resulting in a D/Pd ratio of about 0.7. The Si-Pd pellet is normally pulsed at 500 volts and at a low duty cycle to reduce Joule heating. The pulsing presumably injects electrons from the Si into the Pd and enhances electronic screening in the Pd lattice.

Ten experiments have been conducted. The cells are operated in a neutron counter and tritium assays are performed on the D_2 gas before and after the run. In the early runs, the neutron counting efficiency was low ($\sim 1\%$), and the background was relatively high. In one of these runs, the neutron rate appeared to be

above background and the tritium content of the D_2 gas was about three orders of magnitude greater after the run than before. In recent runs, neutron counting has been performed in a low background environment with 20% detection efficiency, and neither the excess neutrons nor the tritium buildup has been reproduced. A tenth cell is currently in operation. Details are shown in Table 3.

MISCELLANEOUS

A single experiment was performed in which deuterated Pd foil was explosively compressed. Both on-line neutron counters and later counting of activation foils indicated that neutron production was below the limits of detection of either method ($<10^4$ neutrons from the device).

THEORETICAL ACTIVITIES

As discussed in the introductory paragraphs, theorists at Los Alamos have already addressed some aspects of cold-fusion phenomena, and an expanded effort is both in progress and about to bloom.

Results of the fusion reaction rate calculations at very low kinetic energies are shown graphically in Figs. 2 and 3. These calculations have demonstrated the importance of using DT gas in the pressurized gas-metal measurements as an indicator of the reaction temperature and/or kinetics where microscopic "hot fusion" might be occurring. The curves indicate that the D-D and D-T fusion rates are about equal at 50 eV, but for deuteron energies above 300 eV the D-T rates are >100 times the D-D rate. Several analyses of barrier penetration factors for cold-fusion reactions in metal hydrides have shown that, at typical vibrational energies in the lattice (<1 eV), the fusion rate for D-T pairs is much less than for D-D pairs, and both rates are less than the rate for H-D fusion. This is associated with the fact that the reduced mass, which enters the exponent in the penetration factor, is largest for D-T and smallest for H-D. Some early electrolysis experiments at Los Alamos were designed to exploit this fact by using an equal mixture of H_2O and D_2O in the electrolyte and looking for the 5.4-MeV gamma ray from the H-D reaction, without success.

The following is a brief summary of the present cold-fusion research program in the Los Alamos Theoretical Division.

Molecular Physics and Theoretical Chemistry

Early analysis showed the experimental results of Jones, *et al*, and of Fleischmann, Pons, and Hawkins could not be explained as muon catalyzed fusion induced by cosmic rays.

The possibility of the fusion of two deuterons screened by the conduction electrons in a metal is currently being investigated. There is reason to believe that the deuterons are bound by a quasi-one-dimensional electronic motion induced by the presence of the metal lattice. *Ab initio* calculations reveal an unexpected state under these conditions bound with keV energies at internuclear distances of less than 0.1 Bohr. Tunneling integrals calculated from preliminary results yield fusion rates much greater than 1/second for the few "molecules" in this channel. However, much more work is necessary to verify the approximations made about the physics of the molecule/metal system. Although exciting, we emphasize that this work is very speculative and at a primitive stage of development.

The location and distribution of the D atoms within the lattice of the metal electrode is another crucial piece of information that is not known for many D/metal-atom ratios, and considerable effort is being devoted to solving these questions. In progress is the development of a better description of the atomic, molecular, and condensed-matter physics, examining electronic screening of deuterons in Pd and Ti and developing a better understanding of the behavior and quantum-mechanical state of deuterons in metal lattices. The latter involves the parameterization of the D-D interaction potential, determination of deuteron location as a function of D to Pd ratio, and the use of electronic-structure calculations for metal clusters.

Nuclear Theory

Efforts are underway to use R-matrix formalism to calculate absolute reaction rates for hydrogen isotope fusion reactions and to predict branching ratios for D-D reactions at very low deuteron energies. This branching ratio has been estimated by using current charge-independent ^4He R-matrix calculations to very low energies; the proton branch was found to be only slightly enhanced. Further calculations will include nucleon charge exchange mechanisms that, in conjunction with the deuteron charge polarization (the Oppenheimer-Phillips effect), are thought by some to offer the possibility of the strong enhancement of the proton branch reported by several experimental groups here, at Texas A&M University, at the Bhabha Atomic Research Centre, India, at the University of Florida, and at the Institute of Petroleum, Mexico.

Cracks and Defects In Solids

It is difficult to see how a crack-driven acceleration potential could produce the neutron yields observed in the pressurized D_2 gas-Ti metal/alloy experiments.

The problem with reaction-in-flight fusion is that in anything but very hot, low-Z plasmas, multiple Rutherford scattering and ionization decelerate the deuteron so rapidly that its probability of reacting becomes very small. When the small fusion cross section at low energy also is factored in, the probability becomes too small to account for any of the reported experimental observations. Perhaps there are effects in these very special materials that would enhance the reaction-in-flight probability. Channeling is one effect currently under investigation. Other effects will be investigated.

New Energy Times Archive

FLANGE TEST CELL

CERAMIC ID. 1.25 in.
 TOTAL ACTIVE LENGTH 0.44 in.
 THICKNESS OF Pd LAYERS 0.047 in.
 THICKNESS OF Si LAYERS 0.085 in.

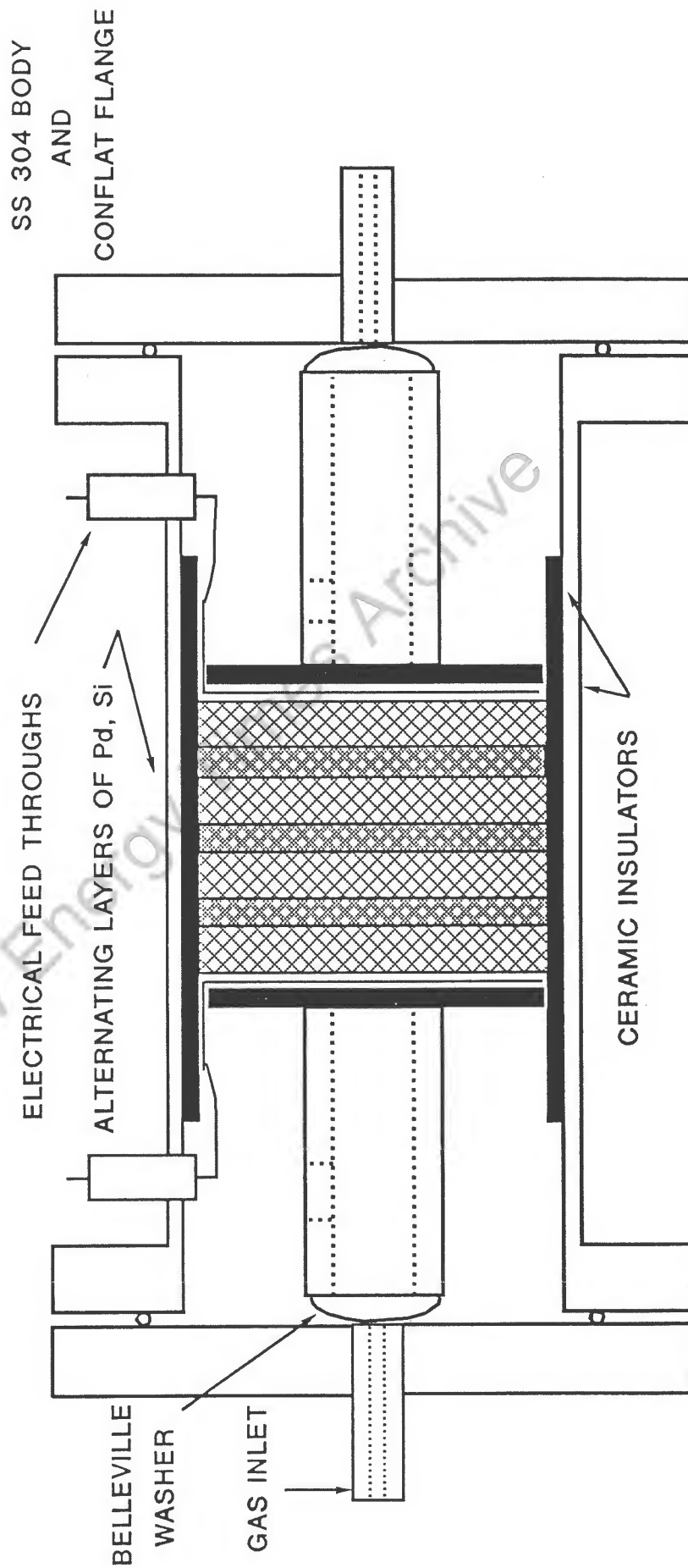


Figure 1.

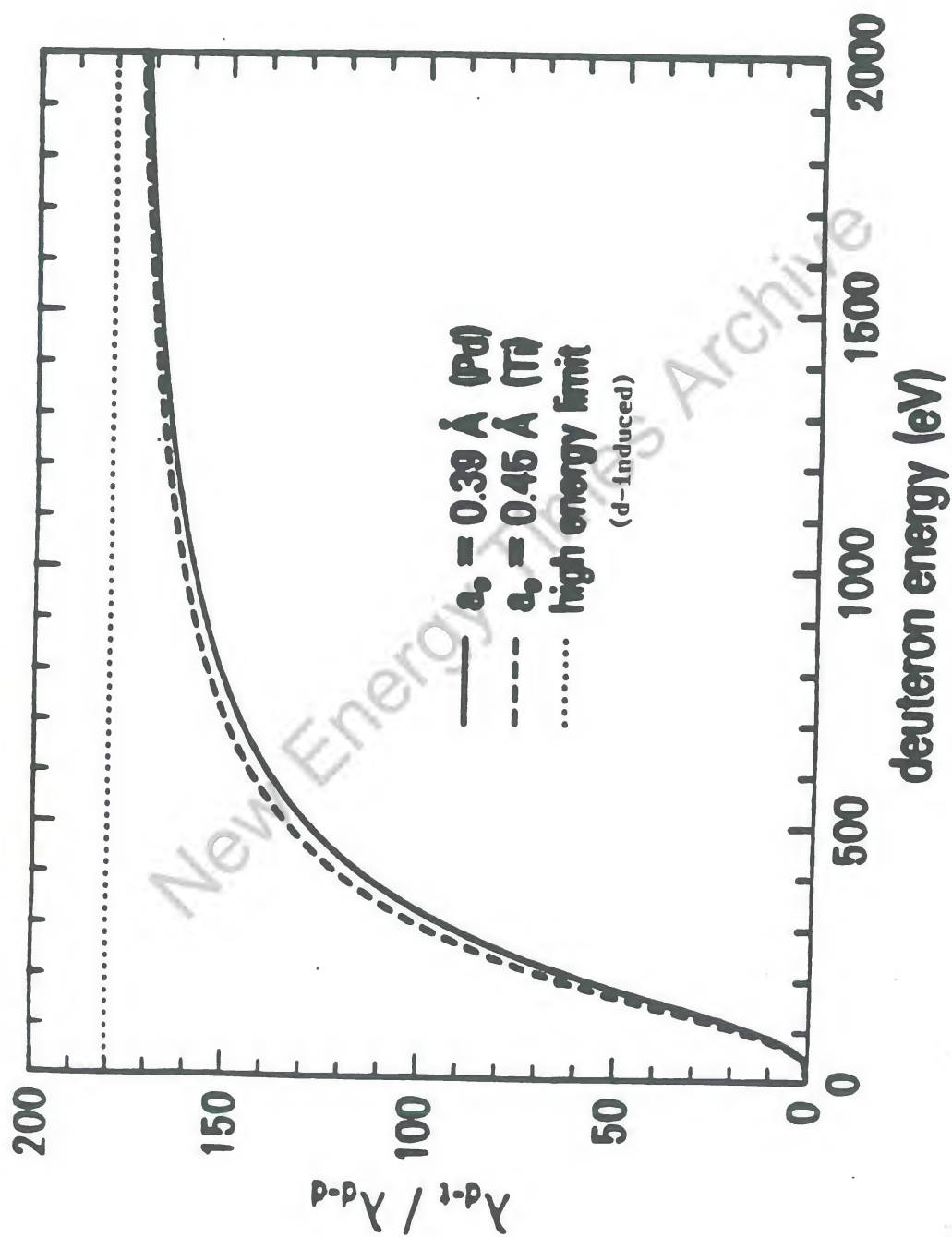


Figure 2.

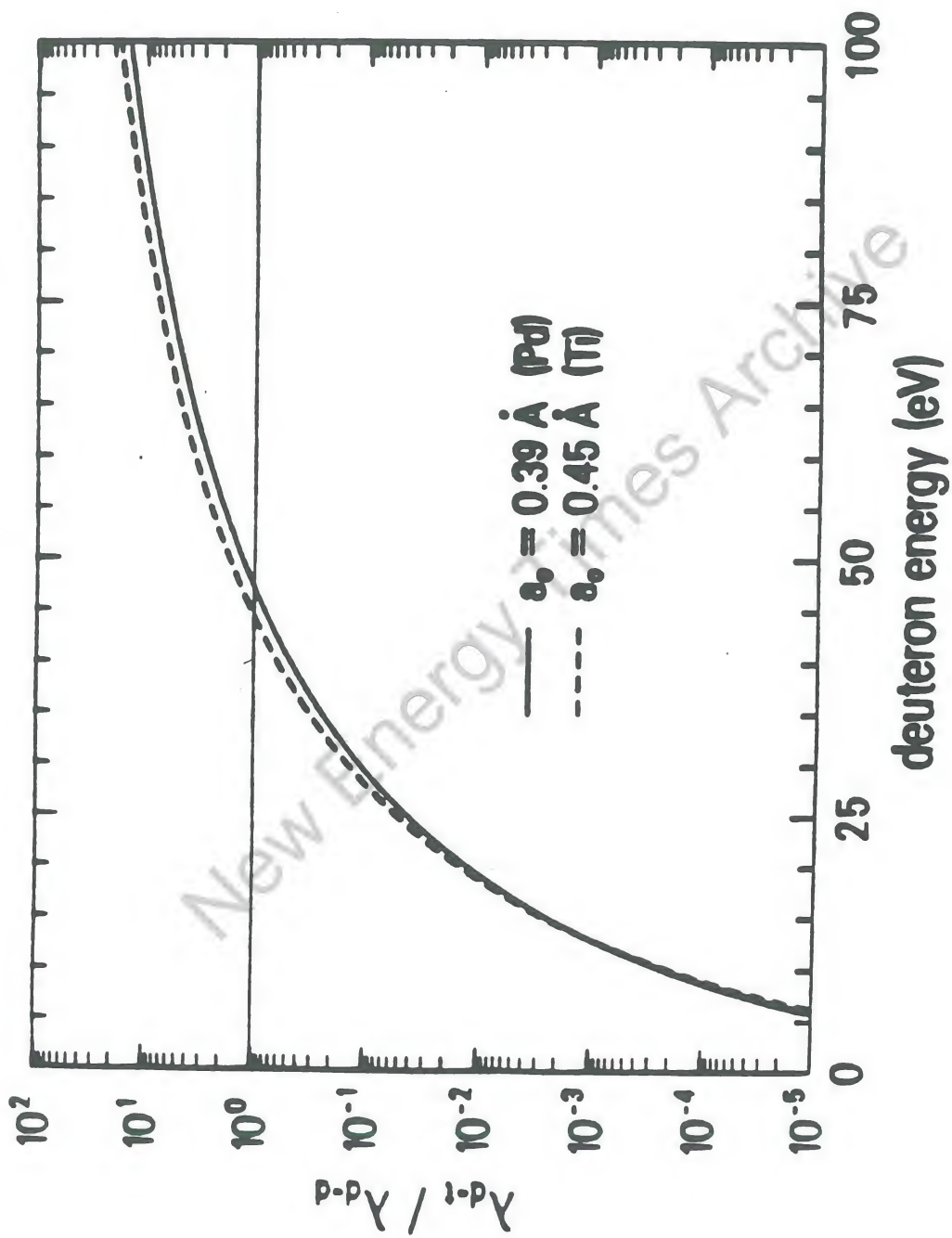


Figure 3.

TABLE 1. Electrochemical Cells

| # | Form | Alloy | Surface Treatment | Pre-Treatment | Electro. Poison | Anode | Container | Epoxy on lead | Max. D/Pd | Date Started |
|----|----------------------|------------|-------------------|-----------------------------------|--------------------------------|----------|-----------|---------------|-----------|--------------|
| | A | B | C | D | E | F | G | H | I | J |
| | A(sc) single crystal | | none | zone melted | none, Cu, Pb | Pt | glass | no | 0.850 | 6/14 |
| | B(sc) single crystal | | none | zone melted | thio, Cu, Pb | Pt | glass | no | 0.810 | 6/19 |
| 2 | coin | Pd+C | std | none | none | Pt | plastic | yes | | 7/2 |
| 4 | button | Pd | none | annealed | none, Cu, Pb | Pt | glass | no | 0.089 | 5/4 |
| 6 | button | Pd+C | C | melted in C | none, Cu, Pb | Pt | glass | no | 0.121 | 5/4 |
| 7 | button | Pd+S | none | none | none, Cu, Pb | Pt | glass | no | 0.680 | 5/4 |
| 8 | button | Pd+C | none | none | none, Cu, Pb | Pt | glass | no | 0.024 | 5/4 |
| 9 | button | Pd | S | H ₂ S | none, Cu, Pb | Pt | glass | no | 0.720 | 5/5 |
| 11 | coin | Pd | S | H ₂ S+C | none, Cu, Pb | Pt | glass | no | 0.880 | 5/9 |
| 12 | coin | Pd | S | H ₂ S+C | none, Cu, Pb | Pt | glass | no | 0.840 | 5/9 |
| 13 | coin | Pd | std | none | none, Cu, Pb | Pt | glass | no | 0.830 | 5/8 |
| 14 | coin | Pd | S,Cu | H ₂ S+C | none, Cu, Pb | Pt | glass | no | 0.800 | 5/10 |
| 15 | coin | Pd | std | anneal | none, Cu, Pb | Pt | glass | no | 0.780 | 5/10 |
| 16 | coin | Pd | Zn | Zn vapor | none, Cu, Pb | Pt | glass | no | 0.800 | 5/12 |
| 17 | sheet | Pt | none | none | none, Cu, Pb | Pt | glass | no | 0.000 | 5/15 |
| 18 | coin | Pd | Cu | plated | none, Cu, Pb | Pt | glass | no | 0.700 | 5/16 |
| 19 | coin | Pd+S | std | none | none, Cu, Pb | Pt | glass | no | 0.660 | 5/16 |
| 20 | coin | Pd+Rh | std | none | NaCN,Cu,Pb | Pt | glass | no | 0.890 | 5/18 |
| 21 | coin | Pd | Ni | none | NaCN,Cu,Pb | Pt | glass | no | 0.690 | 5/19 |
| 22 | coin | Pd | std | none | NaCN,Cu,Pb | Pt | glass | no | 0.840 | 6/1 |
| 23 | coin | Pd | Ni | none | NaCN,Cu,Pb | Pt | glass | no | 0.810 | 5/20 |
| 24 | coin | Pd | std | annealed | none, Cu,Pb | Pt | glass | no | 0.760 | 5/21 |
| 25 | coin | Pd | std | none | none, Cu,Pb | Pd+Au | glass | no | 0.820 | 5/22 |
| 26 | coin* | Pd+Li | std | none | none-thio | Pt | plastic | yes | | 6/1 |
| 27 | coin | Ni | std | none | none | Pt | plastic | yes | 0.090 | 6/1 |
| 28 | coin | Pd+Rh | std | none | thio | Pt | plastic | yes | | 6/2 |
| 29 | coin | Pd | S | H ₂ S+C | thio | Pt | plastic | yes | tritium | 6/5 |
| 30 | coin | Pd | S | H ₂ S+C | none | Pt | plastic | yes | tritium | 6/5 |
| 31 | coin | Pd+Rh+Li | std | none | thio | Pt | plastic | yes | | 6/8 |
| 32 | coin | Pd | std | none | thio | Pt | plastic | yes | | 6/8 |
| 33 | coin | Pd+Li | std | none | none-thio,Cu | Pt | plastic | no | 0.770 | 6/15 |
| 34 | coin | Pd+Li | std | none | none-thio,Cu | Pt | plastic | no | 0.829 | 6/15 |
| 35 | coin | Pd+Li | std | none | none-thio,Cu | Pt | plastic | no | 0.767 | 6/15 |
| 36 | coin | Pd+Rh | std | none | thio,Cu,Pb | Pt | plastic | no | 0.861 | 6/17 |
| 37 | coin | Pd+Rh | std | none | thio,Cu,Pb | Pt | plastic | no | 0.896 | 6/17 |
| 38 | coin | Pd+Rh | std | none | thio,Cu,Pb | Pt | plastic | no | 0.848 | 6/17 |
| 39 | #26 B | Pd+Li | std | none | none | Pt | glass | yes,special | | |
| 40 | coin | Pd | S | H ₂ S+C | none | Pt | plastic | no | 0.835 | 6/20 |
| 41 | wire | Pd, Marsh. | none | none | thio | Pt | plastic | yes | 0.863 | 6/21 |
| 42 | coin | Pd+S | std | none | none | Pt | plastic | yes | | 6/24 |
| 43 | coin | Pd+B | std | none | As ₂ O ₃ | Pt | plastic | yes | | 6/24 |
| 44 | coin* | Pd | S | H ₂ S+C | none | Pt | plastic | yes | 0.745 | 6/26 |
| 45 | coin | Pd | S | H ₂ S+C | none | Pt | plastic | yes | 0.671 | 6/26 |
| 46 | coin* | Pd | S | H ₂ S+C | none | Pt | plastic | yes | | 6/27 |
| 47 | coin* | Pd | S | H ₂ S+H ₂ O | none | Pt | plastic | yes | | 6/30 |
| 48 | coin* | Pd | S | H ₂ S+H ₂ O | none | Pt | plastic | yes | | 6/30 |
| 49 | wire* | Pd+Li | none | none | none | Pt | plastic | yes | | 8/15 |
| 50 | coin | Pd sheet | std | none | none | Pt | plastic | yes | | 7/2 |
| 51 | coin* | Pd sheet | std | annealed | none | Pt | plastic | yes | 0.800 | 7/4 |
| 52 | coin* | Pd+C | Na ₂ S | oxidized | none | Pt | plastic | 1.yes, 2.no | 0.875 | 7/8 |
| 54 | coin* | Pd | std | none | pre-electro. | Pt | plastic | no | 0.770 | 7/31 |
| 55 | coin* | Pd+Li | std | none | pre-electro. | Pt | plastic | no | 0.740 | 7/31 |
| 56 | coin* | Pd+C | Li ₂ S | oxidized | none | Pt | plastic | no | 0.660 | 7/31 |
| 57 | strip* | Pd | none | none | U metal | Pt | plastic | no | | 8/9 |
| 58 | sheet* | Pd | none | none | thio | Pt | plastic | no | 0.830 | 8/9 |
| 59 | sheet* | Pd | none | none | thio | Ni gauze | plastic | no | 0.710 | 8/9 |
| 60 | sheet* | Pd | none | none | Li ₂ S+alcohol | Ni gauze | plastic | no | 0.710 | 8/9 |

TABLE 1. Electrochemical Cells (Continued)

| | | | | | | | | | | |
|----|--------|-------------|------|------------------|--------------|-----------|---------|----|-------|------|
| 61 | sheet* | Pd | none | none | Fe metal | Pt | plastic | no | 0.800 | 8/9 |
| 62 | sheet* | Pd | S | H ₂ S | none | Pt | plastic | no | 0.560 | 8/9 |
| 63 | sheet* | Pd | S | H ₂ S | pre-electro. | Pt | plastic | no | 0.670 | 8/9 |
| 64 | sheet* | Pd | S | H ₂ S | none | Pt | plastic | no | 0.690 | 8/15 |
| 65 | coin* | Pd+C | std | none | none | Pt | plastic | no | 0.770 | 8/15 |
| 66 | strip* | Pd | none | none | none | Ni wire | plastic | no | | 8/22 |
| 67 | strip* | Pd | none | none | none | stainless | plastic | no | | 8/23 |
| 68 | coin* | ultra pure | std | none | none | Pt | plastic | no | 0.790 | 8/30 |
| 69 | coin* | Pd, Engh. | std | none | none | Pt | quartz | no | | 9/5 |
| 70 | wire* | Pd, Martin | none | none | none | Ni wire | glass | no | | 9/5 |
| BB | wire* | Pd, Brokris | none | none | none | Ni gauze | glass | no | | 8/7 |
| BM | wire* | Pd, Martin | none | none | none | Ni gauze | glass | no | | 8/7 |

As of 9/6/89

A * = operating cells

button = arc melted only

coin = arc melted and rolled into coin shape

sheet = 0.05" thick sheet cut into square shape

strip = strip cut from sheet to give 0.05"x0.05"x1" electrode

wire = a cylinder having a diameter from 0.03" to 0.04"

BB, BM = cells identical to those used at Texas A and M

B Alloy made by arc melting Pd with the other component

C Various surfaces applied as described under "D"

std. = sanded with 200 grit paper and washed with nitric acid

none = cleaned with HNO₃ or H₂O₂D H₂S+C = heated in H₂S+paraffin vaporH₂S+H₂O = heated in H₂S that was bubbled through H₂OH₂S = heated in pure H₂S to form Pd sulfide on surface

oxidized = heated in air to produce microfractures on surface

annealed = heated in vacuum

E none, Cu, Pb = some cells picked up Cu and Pb from electrode disconnect assembly

thio = thiourea added to electrolyte

pre-electro. = current was passed through electrolyte using a Pt dummy electrode before Pd was used

F Pt = platinum gauze

Ni wire = nickel wire was made into a spiral (0.3" ID) around the anode

Ni gauze = gauze obtained from Texas A and M

G Glass = flint glass

Plastic = polyethylene

H yes = Pt wire from Pd electrode was covered with Torr Seal to prevent Cu and Pb pickup

I Maximum determined from weight gain

J Month and day cell started

TABLE 2. Pressurized Gas-Metal Experiments

| <u>Run</u> | <u>wt. (g)</u> | <u>material</u> | <u>loading conditions*</u> | <u>results</u> |
|------------|----------------|--|---|---|
| Ti-1 | 100 | Ti sponge | outgassed 150 °C 1 hour backfilled 600 psi D ₂ at room temp | 4 bursts cycles 3,4 low level continuous emission |
| | 4.2 | Ti 6-6-2 turnings | | |
| | 2.1 | Ti crystals | | |
| | 11.0 | Ti sponge cathode | | |
| Ti-2 | 100 | Ti sponge | outgassed 200 °C 1 hour, backfilled at LN temp with 400 psi D ₂ | none |
| | 100 | Ti sponge crystals | | |
| Ti-5 | 46.4 | Ti turnings | outgassed 200 °C 1 hour, backfilled 600 psi D ₂ room temp | none |
| | | | | |
| Ti-6 | 146.9 | Ti pieces | outgassed 200 °C 1 hour backfilled 600 psi D ₂ room temp | 8 bursts, cycles 4-9 P=200 psi at end of experiment, repressurized P=580 psi, no more neutrons |
| | 17.4 | Ti powder | | |
| | 22.8 | Ti sponge cathode | | |
| | 1.7 | Pd pieces | | |
| | 4.9 | Pd powder | | |
| Ti-7 | 33.1 | Ti sponge preduterated at 550 °C (TiD _{0.18}) | backfilled 580 psi D ₂ at room temp | none |
| Ti-8 | 50 | Ti turnings | outgassed 200 °C 580 psi at room temp, D ₂ | none |
| | 4 | Ti sponge | | |
| Ti-9 | 30 | Ti turnings and sponge, 24 hr | outgassed 200 °C 1 hour, backfilled D ₂ | none |

*D₂ gas unless otherwise specified.

TABLE 2. Pressurized Gas-Metal Experiments (Continued)

| | | as cathode, 20 min anode | 580 psi room temp | |
|-------|---------------------------|--|--|----------------|
| Ti-10 | 23 64.5 4 9 | Ti turnings cathode misc. Ti sponge Ti sponge, Pd foil Ti sponge cathode | outgassed 200 °C 1 hour, backfilled 580 psi room temp | small bursts |
| Ti-11 | 82 5 5 | Ti powder Ti 10% Pd powder Ti 10% Pd sintered 900 °C in air | outgassed 200 °C 1 hour, backfilled 580 psi room temp | small bursts |
| Ti-12 | 14.8 | Ti sponge cathode | outgassed 200 °C 1 hour, backfilled 580 psi room temp | small burst |
| Ti-13 | 10.3 | Ti 6-6-2 turnings | degreased with dichloromethane rinsed with methanol normal outgassing | small burst |
| Ti-14 | 60 | Ti 6-6-2 turnings | same as Ti-13 | several bursts |
| Ti-15 | 50 10 10 | Ti sponge oxidized 900 °C Ti turnings PVD Pd coated, oxidized 900 °C Ti turnings PVD Pd coated, cathode | outgassed 200 °C 1 hour, backfilled 550 psi at room temp | none |
| Ti-16 | 30 10.5 3.0 11.4 | Ti sponge cathode Pressed Ti-Pd (80:20) Pd sheet cathode Ti-Pd (90:10) air | outgassed 200 °C overnight deuteriding occurred when cylinder pressurized | 1 large burst |

TABLE 2. Pressurized Gas-Metal Experiments (Continued)

| | | | | | |
|------|--------|--|---|-------------------------------|--|
| | | sintered cathode Ti-Pd (90:10) vacuum sintered cathode Misc. Ti-Pd, Ni, Zr, V cathodes | | | |
| 11.9 | | | | | |
| 42 | | | | | |
| | Ti-16A | same as Ti-16 | refilled with 520 psi | bursts | |
| | Ti-16B | same as Ti-16 | refilled with 500 psi | bursts, large burst at -30 °C | |
| | Ti-16C | same as Ti-16 | refilled 500 psi | none | |
| 60 | Ti-17 | Ti 6-6-2 turnings | outgassed 200 °C 1 hour, backfilled 40 psi | none | |
| 60 | Ti-17A | same as Ti-17 | backfilled 520 psi | none | |
| 60 | Ti-18 | Ti 6-4 turnings | outgassed 200 °C 1 hour, backfilled 520 psi | none | |
| 36 | Ti-19 | Ti 6-4 turnings | outgassed 200 °C 1 hour, backfilled 500 psi | 1 large burst (R=412) | |
| 50 | Ti-20 | Ti 6-6-2 turnings | outgassed 200 °C 1 hour, backfilled 500 psi | none | |
| 27.2 | Ti-21 | Ti-Pd (80:20) N ₂ sintered | outgassed 200 °C 5 hours, backfilled 480 psi (some dueteriding occurred) | none | |
| 17.6 | | Ti-Pd (90:10) air sintered | | | |
| 1.2 | | Zr foil | | | |
| 3.9 | | V foil | | | |

TABLE 2. Pressurized Gas-Metal Experiments (Continued)

| | | | | | |
|--------|-------|---|---|--------------------------------------|--|
| Ti-21A | 63 | Misc cathodes Ti turnings Ti sponge Ti-Pd (90:10) sintered | | | |
| | Ti-21 | same as Ti-21 | refilled with 480 psi | none | |
| | 50 | Ti 6-6-2 turnings | outgassed 200 °C | | |
| | 50 | Ti 6-4 turnings | 2 hours, backfilled 500 psi H ₂ + D ₂ | 1 large burst | |
| | 50 | Ti 6-6-2 turnings | outgassed 200 °C 1 hour, backfilled 480 psi D ₂ | none | |
| | 50 | Ti 6-4 turnings | outgassed 200 °C 1 hour, backfilled 480 psi D ₂ | large burst (-30 °C) small bursts | |
| | 50 | Ti 10-2-3 turnings (V-Fe-Al) | outgassed 200 °C 1 hour, backfilled 460 psi D ₂ | none | |
| | 133 | Ti 6-4 turnings | outgassed 200 °C 1 hour, backfilled 460 psi D ₂ , 240 psi H ₂ | none | |
| Ti-27 | 20 | Ti 6-6-2 turnings | outgassed 200 °C | | |
| | 20 | Ti 6-4 turnings | 1 hour, backfilled 500 psi H ₂ | none | |
| | 20 | Ti 10-2-3 turnings | | | |
| Ti-28 | 50 | Ti 6-6-2 turnings | outgassed 200 °C | | |
| | 33 | Ti 6-4 turnings | 1 hour, backfilled 250 psi D ₂ , 250 psi H ₂ | none | |

TABLE 2. Pressurized Gas-Metal Experiments (Continued)

| | | | | |
|-------|----------|--------------------------------------|--|-------------|
| Ti-29 | 50 50 | Ti 6-6-2 turnings Ti 6-4 turnings | outgassed 200 °C 1 hour, backfilled 500 psi <u>H₂</u> | none |
| Ti-30 | 100 | Ti sponge | outgassed 200 °C overnight, backfilled 460 psi D ₂ | none |
| Ti-31 | 50 50 | Ti 6-6-2 turnings Ti 6-4 turnings | outgassed 200 °C 1 hour, backfilled 500 psi <u>H₂</u> | in progress |

Table 3. Short Sample Histories of Solid State Cells

Sample 1. 4-12, This cell shorted out after deuterium was added to the cell. The cell was tested at LANSCE with 200 V pulses at 50 mW dissipation with no excess heating or neutron activity observed.

Sample 2. 4-14, New ceramic disks and belleville washers were incorporated into the cell design to restrain the expansion of the palladium. The cell was filled with D_2 (110 psia) and used until 4-26 when about 5% H_2 was added to cell. Neutron activity was up to 5 sigma over background and monotonically decreased with operation until H_2 was added to cell. This sample was checked for helium (on 5-20) which was found at normal background levels (15 ppm) and then kept sealed for further analysis. A tritium analysis done on 6-30 found the cell to have 1300 times the tritium background level present in the fill gas. Tritium confirmed in subsequent gas analysis and on stack monitor during initial release.

Sample 3. 4-19, Control sample filled with 110 psia of H_2 . No neutron count rate above background or correlated output found at LANSCE. No excess heating.

Sample 4. 5-3, Vacuum control sample. This sample was filled with the palladium and silicon powder but was evacuated prior to testing at LANSCE. No excess heating or neutron activity observed over background. This sample was then filled to 110 psia of D_2 and tested for neutron activity and heating. Only one burst of neutron activity was seen at the start of a count and no excess heating was observed. Because of a leaky seal, this cell was only tested for 45 minutes at LANSCE.

Sample 5. 5-8, D_2 sample (110 psia) for use in Menlove's laboratory. This sample had a serious D_2 leak and was only tested for 15 minutes with negative neutron and heating results.

Sample 6. 5-30, D_2 sample (110 psia) for use in Menlove's laboratory. This sample shorted (resistance 350 ohms rather than 30K ohms) after it was initially pulsed. This sample had deliberately mixed palladium in the silicon powder layers. No neutron output within statistical error of 2 sigma. Tritium analysis showed 110 micro curies per meter cubed (identical to fill gas bottle within 5%).

Sample 7. 7-18, D_2 sample (106 psia) made with mixed powder layers. Sample showed a 2.5 sigma increase in neutron output when voltage on cell was raised from 480 to 800 volts. Cell was run for 95 hours total. Tritium analysis showed 168 micro curies per meter cubed, slightly over the fill gas value of 110.

Sample 8. 8-9, Sample cell with new flange design (Figure 1) using mixed powders. New sample containment chamber used. Filled with 200 psig of D_2 . Because of Jones's cells the sample was only allotted 18 hours of counter time. No neutron output to within 1 sigma. Tritium level measured to be within 6% of fill gas level of 28 micro curies per meter cubed.

Sample 9. 8-14, Sample same as 8 but outgassed at elevated temperature. Water, carbon monoxide and carbon dioxide as well as some hydrogen were evolved during the vacuum bakeout. Filled with 130 psia of D_2 . No neutron output to within 1.8 sigma and no voltage dependence observed. Tritium to be analyzed.

Sample 10. 9-4, Layered sample in new containment chamber. Filled with 250 psig of D_2 . Extensive measurements in progress in Menlove's channel neutron counter.